A GYROKINETIC ANALYSIS OF ELECTRON PLASMA WAVES AT RESONANCE IN MAGNETIC FIELD GRADIENTS

Darren McDonald

A Thesis Submitted for the Degree of PhD
at the
University of St Andrews

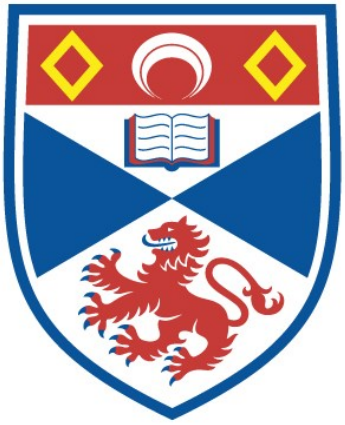

1995

A GYROKINETIC ANALYSIS OF ELECTRON PLASMA WAVES AT RESONANCE IN MAGNETIC FIELD GRADIENTS

DARREN MCDONALD

THESIS SUBMITTED FOR THE DEGREE OF DOCTOR OF PHILOSOPHY OF THE UNIVERSITY OF ST. ANDREWS IN SEPTEMBER 1994

TK

B640

A GYROKINETIC ANALYSIS OF ELECTRON PLASMA WAVES AT RESONANCE IN MAGNETIC FIELD GRADIENTS

ABSTRACT

To produce nuclear fusion in a Tokamak reactor requires the heating of a plasma to a temperature of the order of 10 keV. Electron cyclotron resonant heating (ECRH), in which the plasma is heated by radio waves in resonance with the Larmor frequency of the plasma's electrons, is one scheme under consideration for achieving this.

A description of such a heating scheme requires a theory to explain the propagation and absorption of high frequency waves in a plasma in the presence of a magnetic field gradient. A WKB analysis can describe some of the processes involved but a complete explanation requires the use of full wave equations.

In this thesis we shall develop a technique for deriving such equations which will be shown to be simpler and more general than calculations performed by earlier workers. The technique relies on including the effect of the magnetic gradient across the Larmor orbit of the electrons in the resonance condition of the wave, the so called Gyrokinetic correction, which has been ignored in calculations by previous workers.

Once derived, the equations are solved numerically and the results applied to a number of experiments currently being performed on Tokamak fusion.

In addition, we shall also look at the energy loss processes of runaway electrons, which have been shown experimentally to be shorter than would be expected.

DECLARATION

I, D.C. McDonald, hereby certify that this thesis, which is approximately 20 000 words in length, has been written by me, that it is a record of work carried out by me and that it has not been submitted in any previous application for a higher degree.

date 30/9/94 signature of candidate

POSTGRADUATE CAREER

I was admitted as a research student in October 1990 and as a candidate for the degree of Doctor of Philosophy in the same month; the higher study for which this is a record was carried out in the University of St. Andrews between 1990 and 1994.

date 30/9/94 signature of candidate

CERTIFICATE

I hereby certify that the candidate has fulfilled the conditions of the Resolution and Regulations appropriate for the degree of Doctor of Philosophy in the University of St. Andrews and that the candidate is qualified to submit this thesis in application for that degree.

date signature of supervisor

COPYRIGHT

ACKNOWLEDGEMENTS

I first visited St. Andrews just over seven years ago and fell immediately in love with the town. Little has changed since then to alter my opinion and so I begin by thanking St. Andrews, the town and the University, for providing an environment in which I have been able to grow, both academically and in character. A special thanks goes, of course, to all the friends I have made here as both an Undergraduate and Postgraduate student.

Thanks too to my colleagues and friends in the Department of Mathematics for their support and assistance and for making my time as a postgraduate such a happy one. In particular, I'd like to thank Dr Patricia Heggie, for her help with all things computational, Dr Rekha Jain for her final reading of this thesis, and the members of the Plasma Physics group; Professor Jeffrey Sanderson, Dr Helen Holt, Michael Taylor and David Johnson.

Throughout my time as a postgraduate I was funded by the Science and Engineering Council, to whom I will be eternally grateful, and by the United Kingdom Atomic Energy Authority, who I also thank, not least because my work with them provided many interesting visits to their laboratories at Culham. At Culham, I extend my gratitude to all those who helped me in the many fruitful discussions I had there. In particular I wish to thank Julie Bishop, Dr Kin Kam, Dr Brian Harvey and Dr Doug Bartlett. Most of all, however, my thanks go to Dr Chris Lashmore-Davies for his advice, enthusiasm and for sharing his knowledge of all areas of the field of fusion research.

Finally, I would like to thank my supervisor Professor Alan Cairns for his continual guidance and help and, above all, for his patience and encouragement throughout the final writing up of this thesis.

To my parents

TABLE OF CONTENTS

APPENDIX

A SPECIAL FUNCTIONS.

1. INTRODUCTION

1.1 Review of Nuclear Fusion.

Fusion power is expected to be a significant contributor to the world's energy supply in the next century. However, many problems have still to be overcome before efficient commercial reactors can be built. One such problem is the heating of the reactants to the high temperatures required for fusion, in a controlled way.

By the year 2050 estimates suggest that population growth combined with economic development, particularly in third world countries, will lead to at least a doubling of the world's energy demands. Fusion power is expected to be a major source of this energy. Unlike fossil fuels (coal, oil and gas) its fuel (hydrogen) is abundant and easily available, through the electrolysis of sea water. Perhaps, though, fusion's main advantage is its limited impact on the environment. Fusion does not produce the large carbon dioxide and sulphur emissions created by burning fossil fuels and any radioactive waste produced does not require isolation on the geological time scales associated with nuclear fission.

Nuclear fusion is the generation of power by the fusing of two hydrogen nuclei to make helium. Currently, the most favoured reactor design for achieving this is a tokamak, which consists of a hot hydrogen plasma confined by a magnetic field. A plasma, the so called fourth state of matter, is a heavily ionized gas consisting of ionized molecules and free electrons as well as the neutral atoms and molecules common to normal gases. The physics of tokamak plasmas is dominated by the interaction of the plasma with magnetic fields.

Essentially, when a charged particle is placed in a strong magnetic field it becomes tied to a field line, travelling in a spiral trajectory along it. In a toroidal confinement device, field coils are used to produce a circular magnetic field (known as the toroidal field) around which the charged particles of a plasma will travel in their spiral trajectories. In this way the plasma is confined by the magnetic field. In practice, however, the gradient of the magnetic field (which decreases radially) results in the plasma particles drifting away from the field lines and so the plasma becomes unstable. The tokamak overcomes this by using a toroidal current generating a poloidal component to the confining magnetic field, resulting in field lines that spiral around the torus. In this the plasma particles spend equal amounts of time in areas of high and low magnetic field, and as a result the effects of the magnetic field gradient are neutralised. This then is the basic design of all tokamaks: a toroidal vessel surrounded by poloidal field coils, for generating the toroidal field, and toroidal field coils for inducing the toroidal current in the plasma. Although other schemes for plasma confinement have been tried (for example mirrors, pinches and, most notably, inertial confinement) tokamaks are now the most favoured design.

The major problems in tokamak design are confinement and heating. Confinement concerns the containment of the fusion plasma inside the vessel for a period of time long enough for a significant amount of energy to be extracted from it. Plasmas seem to be, by nature, extremely unstable and so the problems of confinement are innumerable (see White (1989)), although there has been much experimental success in this area in recent years. The problems of heating, which are the concern of this thesis, involve raising the temperature of the plasma to a state at which fusion will occur (around 15 keV) and a variety of schemes have been put forward for achieving this.

The criteria for achieving fusion are that the pressure and temperature be high enough for fusion to occur and that the confinement time (effectively the cooling time of

the plasma through thermal conduction) be long enough that net energy is produced by the reactor. More precisely, we require that the ion temperature is at least 10 keV and that the product (known as the fusion product) of the ion density, the ion temperature and the confinement time is at least 3 x 10^{21} m^{-3} keV s. Individually, the predicted targets for the three parameters are given in table 1.1.

Table 1.1

Targets for nuclear fusion

Ion Temperature	15 keV
Density	2 x 10^{20} m^{-3}
Confinement time	1s

Experimental reactors have already come close to reaching the required temperature and confining the plasma at sufficiently high densities. However, no experimental reactor has yet reached the required temperature and pressure whilst maintaining a sufficiently long confinement time. The most successful reactor, so far, is JET (the Joint European Torus) and its best pulse so far has been around 20% of what is required for fusion. As the confinement time scales according to the square of the major radius, the production of a break even plasma should require only the building of a large enough reactor. As a result a larger experimental reactor, ITER (the International Tokamak Experimental Reactor), is currently being planned which should produce conditions near to those required for fusion.

1.2 Tokamak Heating Schemes.

Any heating scheme used in a fusion tokamak must satisfy certain basic criteria. Firstly, it must be capable of heating the plasma to fusion temperature (T~15keV) and do

so in an economical way. Secondly, it must introduce the minimum amount of impurities into the reactor vessel as these invariably destabilize the fusion plasma. Further considerations, in selecting one system over another, are the extent to which heating can be localised in the plasma - primarily because heating is required principally at the plasma core, but also because systems of localised heating may be used to control the plasma's thermal profile, hence providing a mechanism for stabilising the plasma - and also whether the system can be used to induce a toroidal current in the plasma necessary to produce the poloidal magnetic field.

Many heating schemes are all ready in use in experimental reactors around the world of which the main ones are,

(1) Ohmic heating

(2) Neutral beam

(3) Radio frequency heating

which are usually used in some combination.

Ohmic heating is perhaps the most straightforward, but has a limited heating ability. As discussed in section 1.1, tokamaks require a toroidal current to stabilise the plasma. The resistance of the plasma to this current means that this naturally results in the plasma being heated ohmically. However, as the resistance of the plasma goes with temperature as $T^{-3/2}$, such a heating scheme becomes less and less effective as the temperature rises. In practice, ohmic heating can only be used up to a maximum temperature of around 3-4 keV. However, ohmic heating is invariably the first stage of any scheme with other schemes being seen as auxiliary heating to this.

Neutral beam heating is an effective way of heating a plasma, it has no upper limits on temperature, but suffers from its introduction of impurities into the plasma. It involves the bombarding of the plasma with a beam of high energy neutral atoms, which exchange their energy with the plasma through collisions. Its simplicity and effectiveness made it a popular scheme, particularly in the early tokamak experiments. However, in general we find that a significant number of the neutral atoms pass straight through the plasma and strike the reactor vessel on the far side. This results in the removal of atoms from the vessel and, hence, the introduction of impurities into the plasma. In addition it has little possibility for controlling the plasma's thermal profile.

Radio frequency heating (see Cairns (1991)), particularly at ion cyclotron frequencies, is currently the most favoured form of auxiliary heating and is used, to some extent, in most tokamak experiments around the world. It involves the launching of radio waves, from an antenna or waveguide, into the plasma, which is then absorbed by some resonance. Heating schemes have been used experimentally at a number of different frequencies which can be grouped as follows.

Table 1.2

Radio frequency heating schemes

Scheme	**Frequency range**
Alfven wave	1-5 MHz
Ion cyclotron	20-100 MHz
Lower Hybrid	1-5 GHz
Electron Cyclotron	30-150 GHz

Alfven wave heating is perhaps the least successful of the radio frequency heating schemes. In such a heating scheme, a fast Alfven wave is launched into the plasma where

it is converted, at some point, to a slow Alfven wave. Slow (or shear) Alfven waves are, by nature, tied to a magnetic field line and so must then propagate solely within the plasma. Experimentally, though, it has been shown that little energy can be provided by this method (see for example Shohet, 1978). This is believed to be due to a poor coupling between the antenna and the plasma, resulting in little energy reaching the plasma at all.

Ion cyclotron heating, on the other hand, is perhaps the most successful system used thus far, involving the launching of ion cyclotron waves into the plasma which are then absorbed through resonance with the Larmor frequency of the ions. The technology to produce large amounts of power at the required frequencies (a few tens of MHz) is already available and many experiments have successfully used it as a heating scheme (JET has a 16 MW ion cyclotron heating system and ITER is expected to use such a scheme). It also has the advantage that it heats the ions, the particles required for fusion, directly rather than through some collisional process. A more detailed account, of both the theory and experiment, can be found in Swanson (1985).

Lower hybrid heating schemes have also proved successful in some experiments, but is favoured more as a system for current drive. In such a scheme, a wave is launched into the plasma around the lower hybrid frequency (a few GHz) and is then absorbed by Landau damping (a resonance between the wave and the parallel velocity of the electrons). Although such schemes have proved successful in some experiments, some problems have still to be overcome with regard to the propagation of lower hybrid waves through the edge plasma. Certainly, successes in the use of lower hybrid waves for current drive mean that much more research will be done in this area.

Electron cyclotron heating involves the highest frequencies of all Radio frequency heating schemes (typically of the order of tens of GHz). Technically, we are now in the microwave range of frequencies and the new technology required to build devices for

delivering large amounts of power at such high frequencies has hampered all such heating schemes. However, the development of gyrotrons (see Kreischer et al, 1985) in recent years have made such schemes more feasible. Electron cyclotron heating, involves the absorption of radio frequency power by resonance with the Larmor frequency of the electrons. This has a number of advantages over the other schemes with the most important being the simplicity of the coupling between the wave guide and the plasma. Electron cyclotron waves propagate in a vacuum, unlike the lower frequency waves which are evanescent and so lose energy before entering the plasma. As a result, electron cyclotron heating schemes do not require the complicated antenna structures typical of the lower frequency systems. Electron cyclotron heating also provides a strongly localised power deposition which make it ideal for profile control. A good review of the field is given by Bornatici (1983).

Electron cyclotron heating, and in particular the effects upon this of inhomogeneities in the toroidal magnetic field, will be the prime concern of this thesis. We consider then, using electron cyclotron heating as a scheme for heating a tokamak to a temperature at which fusion can take place. Many tokamak experiments are currently underway around the world, of which the largest is the JET experiment in England. As a consequence, we shall take our typical parameters as those of JET which are given in table 1.3.

Table 1.3

Typical JET Parameters

Magnetic Field	2.7 T
Major radius	3 m
Central electron density	2×10^{19} m^{-3}
Central electron temperature	5 keV
Plasma Current	1 MA

1.3 Outline of Thesis.

The core of this thesis is the derivation of full wave equations, to describe electron cyclotron resonance, by the inclusion of the gyrokinetic correction of Lashmore-Davies and Dendy (1989) in a relativistic calculation.

In chapter 2 we give a review of the available theory and discuss its applicability and limitations. In the process, we also introduce important considerations such as ordering and accessibility of the resonances in a natural way. Most importantly, through our discussions of the limitations of the current theory we argue the case for the necessity of a full wave calculation.

In chapter 3 we derive the general full wave equation. This takes the form of a second order integro-differential equation, the solution of which, even by numerical methods, is extremely complex. However, by noting the ordering discussed in chapter 2 we give a method for expanding the equation into a set of differential equations whose solution is considerably simpler.

In chapter 4 we perform such expansions for a number of wave modes and resonances that are of particular interest to us. We then compare the simplicity of our derivation, favourably, with that used previously by Maroli et al (1986).

The self-consistency of the equations produced by our method is best illustrated by their satisfying of energy conservation relations. We illustrate this in chapter 5 by calculating the energy conservation relation for one of the equations in chapter 4. In doing so we also come across the phenomenon of local emission.

Chapter 6 concerns the numerical solutions of the equations of chapter 4, applying them to the COMPASS experiment and the ECA diagnostic in the JET pumped divertor.

Throughout the thesis we restrict our geometry to a simple slab model. However, to extend our technique to more complex geometries, such as the toroidal geometry required for an exact treatment of tokamak heating, would require the use of a more flexible treatment such as that given by the gyrokinetic theory (see Rutherford and Frieman (1968) and Taylor and Hastie, 1968). In chapter 7 we show how to include the gyrokinetic correction in the formalism of relativistic gyrokinetic theory of Tsai et al (1984), and so extend our analysis into more realistic geometries.

In chapter 8 we bring together all our results, obtained in the first seven chapters, and discuss them in the context of present theory and experiment.

Finally, in chapter 9, we present an additional piece of work on runaway electrons and the role of cyclotron instabilities in their energy loss times. This has particular bearing on the understanding of post disruption discharges in JET.

2. PLASMA WAVES.

The description of waves in plasmas is a large subject and many books have been dedicated to it (for example Chen (1987), Swanson (1989) or Stix (1992)). Here we shall concern ourselves with electron cyclotron frequency waves (i.e. ones in which ion effects can be ignored) and give a brief discussion of the models available to describe them along with their respective uses and limitations. We will show that although analysis by cold plasma theory or WKB theory will describe some of the properties of waves in an inhomogeneously magnetised plasma, for a complete description of absorption and mode conversions we must derive the full wave equation.

2.1 Homogenous Plasmas.

We look first at waves in a homogenous plasma (i.e. ones with no magnetic gradient) as their analysis is the simplest and many of the properties exhibited by them are also exhibited, in a modified form, in inhomogenous ones.

The first step in all the analyses is to take an equilibrium plasma and inject into it a small perturbation which is harmonic in space and time (i.e. first order terms go as $\exp(i\mathbf{k}\bullet\mathbf{r} - i\omega t)$). We then take the linearised equation of motion for the plasma (which will vary from model to model) and solve it self-consistently with Maxwell's equations, which now become,

$$\mathbf{k}\times\mathbf{k}\times\mathbf{E}_1 + i\omega\mu_0 \mathbf{J}_1 + \frac{\omega^2}{c^2}\mathbf{E}_1 = \mathbf{0}\,, \tag{2.1}$$

The equation of motion of the plasma is then solved for the perturbed current density ($\mathbf{J_1}$) in terms of the perturbed electric field ($\mathbf{E_1}$) and the result is substituted into (2.1) to give a wave equation for $\mathbf{E_1}$.

2.1.1 Cold Plasma waves.

For a cold plasma we assume that the electrons have no thermal motion of their own and simply behave as a fluid with velocity distribution $\mathbf{v}(\mathbf{x},t)$. The equation of motion of the fluid is,

$$\frac{\partial \mathbf{v}}{\partial t} + (\mathbf{v} \bullet \nabla)\,\mathbf{v} = \frac{q}{m}\left(\mathbf{E} + \mathbf{v} \times \mathbf{B}\right), \tag{2.2}$$

which is linearised and solved in terms of $\mathbf{E_1}$. Using the expression for the conductivity tensor, $\mathbf{J_1} = q\mathbf{v_1}$, we can express Maxwell's equation in the form $\mathbf{D}(\omega,\mathbf{k})\bullet\mathbf{E_1}(\omega,\mathbf{k}) = \mathbf{0}$ (see for example Swanson (1989) or Stix, 1992), where the matrix $\mathbf{D}$ is given by,

$$\mathbf{D} = \begin{bmatrix} S - N^2\cos^2\theta & iD & N^2\cos^2\theta\sin^2\theta \\ -iD & S - N^2 & 0 \\ N^2\cos^2\theta\sin^2\theta & 0 & P - N^2\sin^2\theta \end{bmatrix} \tag{2.3}$$

where,

$$S = 1 - \frac{\omega_p^2}{\omega^2 - \Omega^2}, \qquad D = -\frac{\omega_p^2\Omega}{\omega(\omega^2 - \Omega^2)}, \qquad P = 1 - \frac{\omega_p^2}{\omega^2}$$

$$\Omega = \frac{B_0 q}{m}, \qquad \omega_p^2 = \frac{n_0 q^2}{\varepsilon_0 m}, \qquad N = \frac{k c}{\omega},$$

Without loss of generality, we have taken the magnetic field to lie in the z-direction and θ as the angle between the background magnetic field ($\mathbf{B_0}$) and the wave vector ($\mathbf{k}$). Ω is the electron cyclotron frequency (the Larmor frequency of the electrons about $\mathbf{B_0}$), ω_p is the plasma frequency and N is the refractive index.

For non-trivial solutions we require the determinant of the matrix $\mathbf{D}$ to be zero. This gives us an expression of the form $D(\omega,\mathbf{k}) = 0$ known as the dispersion relation. The solution of this equation gives us the normal modes of the plasma.

If we consider only perpendicular propagation ($\theta = \pi/2$) then the wave equation has the particularly simple form,

$$\begin{bmatrix} S & iD & 0 \\ -iD & S - N_\perp^2 & 0 \\ 0 & 0 & P - N_\perp^2 \end{bmatrix} \begin{bmatrix} E_{1x} \\ E_{1y} \\ E_{1z} \end{bmatrix} = \mathbf{0}. \qquad (2.4)$$

The equation for E_{1x} and E_{1y} has decoupled from the equation for E_{1z}, and we now have two clear solutions; the ordinary mode (or O-mode), where $E_{1x} = E_{1y} = 0$, and the extraordinary mode (or X-Mode), where $E_{1z} = 0$.

For the ordinary mode only E_{1z} is non-zero, and so we have a transverse mode which has dispersion relation,

$$k_\perp^2 c^2 = \omega^2 - \omega_p^2 . \qquad (2.5)$$

A wave will propagate in this mode providing $\omega > \omega_p$.

The extraordinary mode is a partly transverse, partly longitudinal mode, as E_{1x} and E_{1y} are non-zero, and has dispersion relation,

$$k_\perp^2 c^2 = \frac{(\omega^2 - \omega_p^2)^2 - \Omega^2\omega^2}{\omega^2 - \omega_p^2 - \Omega^2}. \qquad (2.6)$$

There is a resonance ($k_\perp \to \infty$) at $\omega^2 = \omega_p^2 + \Omega^2$, which is known as the upper-hybrid resonance, and a cutoff ($k_\perp \to 0$) at $(\omega^2 - \omega_p^2)^2 = \Omega^2\omega^2$. To describe propagation in this mode we use the CMA diagram (Fig (2.1)) in which we plot the variable $X = \omega_p^2/\omega^2$ against $Y = \Omega^2/\omega^2$.

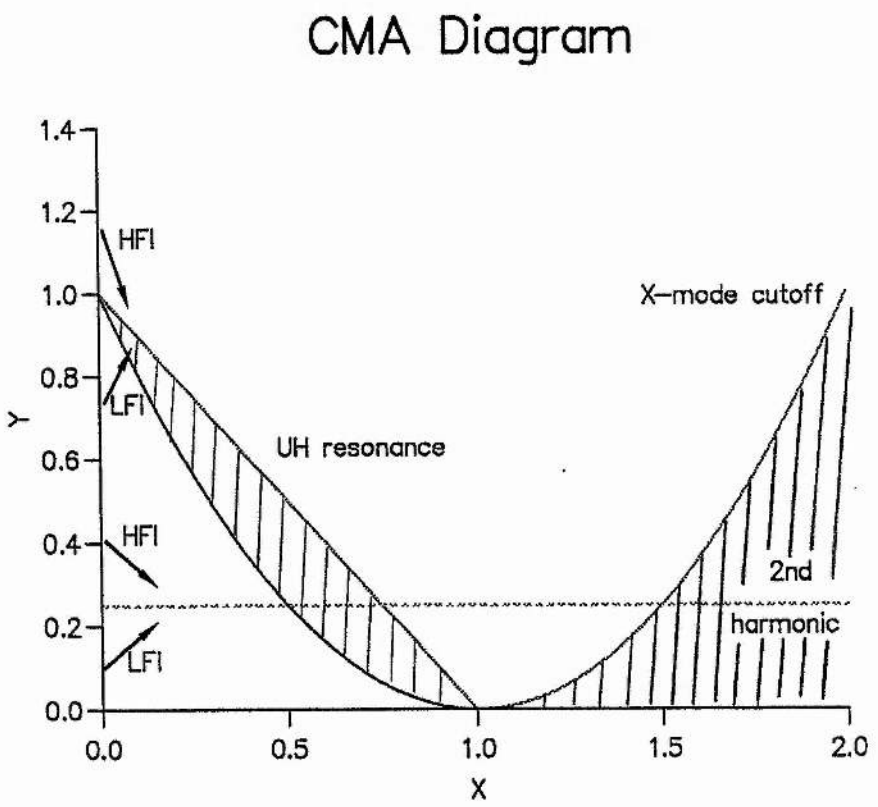

Figure 2.1

CMA diagram for perpendular X-mode

The upper-hybrid resonance is described by the line $Y=1-X$ and the cutoff by the parabola $Y=(1-X)^2$. The wave can only propagate when $k^2 > 0$,which is represented on the diagram by the unshaded region, with the shaded region representing the conditions in which the wave is evanescent ($k^2 < 0$) and hence non-propagating.

In summary, cold plasma theory describes the basic properties of the normal modes of a plasma. However, the theory does not predict the existence of cyclotron resonances, and so cannot predict the propagation of waves through them. To describe this we must consider microscopic effects using kinetic theory.

2.1.2 Waves in a Hot Plasma.

We now consider a hot collisionless plasma, taking into account the microscopic motion of the electrons using kinetic theory.

In kinetic theory we describe the plasma by the distribution function $f(\mathbf{r},\mathbf{v},t)$. The basic equation of motion, for a collisionless plasma, is the Vlasov equation,

$$\frac{\partial f}{\partial t} + \mathbf{v} \bullet \frac{\partial f}{\partial \mathbf{r}} + \frac{q}{m}\left(\mathbf{E} + \mathbf{v} \times \mathbf{B} \right) \bullet \frac{\partial f}{\partial \mathbf{v}} = 0 , \qquad (2.7)$$

which must be solved along with Maxwell's equations. A plasma in thermal equilibrium will have a Maxwellian velocity distribution given by,

$$f_0(\mathbf{r},\mathbf{v},t) = n_0 \pi^{-3/2} v_t^{-3} \exp(-v^2/v_t^2) , \qquad (2.8)$$

where v_t is the thermal velocity of the plasma. Taking this as our unperturbed distribution function we can then solve the linearised Vlasov equation along with Maxwell's equations (2.1) to give (see for example Cairns (1985) or Swanson, 1989),

$$\mathbf{D}(\omega,\mathbf{k}) = \frac{c^2}{\omega^2}(\mathbf{kk} - k^2\mathbf{1}) + \mathbf{1} + \frac{\omega_p^2}{\omega^2}\frac{\omega}{k_z v_t}\exp(-\lambda)$$

$$\times \sum_{n=-\infty}^{\infty} \begin{bmatrix} \frac{n^2 I_n Z}{\lambda} & -in(I_n'-I_n) Z & \frac{n I_n Z'}{(2\lambda)^{1/2}} \\ in(I_n'-I_n) Z & \left(\left(\frac{n^2}{\lambda}+2\lambda\right)I_n - 2\lambda I_n'\right)Z & \frac{\lambda^{1/2}(I_n'-I_n) Z'}{2^{1/2}} \\ \frac{n I_n Z'}{(2\lambda)^{1/2}} & \frac{\lambda^{1/2}(I_n'-I_n) Z'}{2^{1/2}} & I_n Z \end{bmatrix}$$

(2.9)

where, the modified Bessel functions have arguments $\lambda = k^2\rho^2/2$ and $\rho = v_t/\Omega$ is the mean Larmor radius of the electrons, with v_t being the thermal velocity of the electrons. The plasma dispersion functions (PDF's. represented by the Z's in equation (2.9)) have argument $\xi_n = (\omega - n\Omega)/k_z v_t$. What we have now, is a dispersion relation that contains a whole series of cyclotron resonances (with resonance condition $\omega = n\Omega$) with absorption occuring at each one. The PDF's represent the absorption broadening about the cyclotron resonances, which can be illustrated by an analysis of the resonance condition.

$$\omega = n\Omega + k_z v_z \qquad (2.10)$$

which will produce a symmetric absorption broadening with a width on the scale of,

$$\frac{\delta\omega}{n\Omega} \sim N_z \frac{v_t}{c}. \qquad (2.11)$$

For all cases of interest the Larmor radius of the electrons is much smaller than the wavelength and we can use this ratio (ε) as an expansion parameter. This gives the following ordering,

$$k\rho \sim \varepsilon \qquad \text{and} \qquad \lambda \sim \varepsilon^2 . \qquad (2.12)$$

Expanding the dispersion relation in this parameter considerably reduces the complexity of the expression. For example if we take the ordinary mode at perpendicular incidence we have,

$$\left(- k_\perp^2 + \frac{\omega^2 - \omega_p^2}{c^2} \right) - \frac{1}{4} k_\perp^2 \rho^2 \frac{\omega_p^2}{c^2} \frac{\omega}{\omega - \Omega} = 0 . \qquad (2.13)$$

Here, the first bracketed terms are the same as in cold plasma theory and the final term is due to the resonance.

2.1.3 Waves in a Relativistic Plasma.

In a tokamak, electrons are moving at speeds which are an appreciable fraction of the speed of light (e.g. 15% in JET) although still some way below it (the so called weakly relativistic condition). This means that they experience a relativistic mass increase which will affect their behaviour. Most importantly, it affects the resonance condition which now becomes $\omega = n\Omega/\gamma$ (where $\gamma = (1 - v^2/c^2)^{-1/2} \sim 1 + v^2/2c^2$). To produce wave equations which account for such effects we must take the relativistic Vlasov equation,

$$\frac{\partial f}{\partial t} + \frac{1}{\gamma}\mathbf{u} \bullet \frac{\partial f}{\partial \mathbf{r}} + \frac{q}{m_0}\left(\mathbf{E} + \frac{1}{\gamma}\mathbf{u} \times \mathbf{B} \right) \bullet \frac{\partial f}{\partial \mathbf{u}} = 0 , \tag{2.14}$$

where $\mathbf{u} = \gamma \mathbf{v}$, along with Maxwell's equations (2.1). This was first done independently by Dnestrovskii (1964) and Shkarofsky (1966). For the ordinary wave at the fundamental they obtained,

$$-\left(1 + \frac{1}{2}\frac{\omega_p^2}{\Omega^2} F_{7/2}\left(\mu \frac{\omega - \Omega}{\omega} \right) \right) k_\perp^2 + \frac{\omega^2 - \omega_p^2}{c^2} = 0 , \tag{2.15}$$

where $\mu = 2c^2/v_t^2$, that is to say the ratio of the rest mass to the kinetic mass.

The relativistic plasma dispersion function ($F_{7/2}$, see Appendix) represents the spreading of the resonance due to the relativistic mass shift. In a similiar fashion to the Doppler broadening we can look at some of the properties of relativistic mass broadening through its dispersion relation, which is,

$$\omega = n\Omega/\gamma . \tag{2.16}$$

This results in an asymmetric absorption profile, as resonance can only occur at frequencies at or above the cyclotron frequency, on the scale of,

$$\frac{\delta\omega}{n\Omega} \sim \frac{1}{\mu} . \tag{2.17}$$

For non-perpendicular propagation, we would have a combination of both the Doppler and relativistic mass broadening. Comparing the absorption widths from (2.11) and (2.17), we see that we have three different regimes for differing angles of incidence.

For angles close to perpendicular, defined by,

$$| N \cos \theta | << \frac{v_t}{c}, \tag{2.18}$$

we have the quasi-perpendicular regime in which relativistic broadening dominates and we may ignore Doppler broadening effects. For angles sufficiently far from perpendicular, defined by,

$$| N \cos \theta | >> \frac{v_t}{c}, \tag{2.19}$$

we have the opposite case of oblique propagation, in which the Doppler broadening dominates and we may ignore the relativistic effects. In between these two we have a third regime,

$$| N \cos \theta | \sim \frac{v_t}{c}, \tag{2.20}$$

in which both Doppler and relativistic mass effects are important and must be included in any analysis.

2.2 Inhomogenous Plasmas.

For inhomogenous plasmas, such as in a tokamak, the analysis becomes more complicated. We must consider that macroscopic variables (such as the magnetic field, density or temperature) vary spatially. In particular we must consider plasmas with magnetic field gradients which will result in resonances occurring only in restricted regions of the plasma.

If we take a plasma with a magnetic field in the z-direction and a gradient in the x-direction given by,

$$\mathbf{B_0}(x) = B_0(0)\,(1-x/L)\,\mathbf{e_z}\,, \tag{2.21}$$

then, if we take $\omega = n\Omega(0)$, our resonance condition (2.16) gives us an absorption width (δ) which , from (2.17), is of order,

$$\delta \sim \delta\omega\, L \sim \frac{L}{\mu}\,. \tag{2.22}$$

To describe wave propagation in a plasma with a magnetic field gradient requires a considerable increase in complexity. However, if we assume that the scale of the magnetic gradient is much greater than the wavelength we may use WKB theory to apply equations similiar to the homogenous ones.

2.2.1 The WKB Theory.

WKB theory relies upon making the WKB approximation of geometrical optics, namely that the waves travel in single independent modes whose wavelength changes slowly in space, where here we have taken such changes as being in the x-direction. If this is the case we may express perturbed quantities, such as the perturbed electric field, by,

$$\mathbf{E_1}(x) = \mathbf{E_1}\,\exp\left(i\int^{x} dx'\,k(x')\right), \tag{2.23}$$

where we assume that k(x) is slowly varying in that,

$$\frac{1}{k}\frac{dk}{dx} << k\,. \qquad (2.24)$$

In this case we reproduce equations of the same form as Dnestrovskii (1964) and Shkarofsky (1966) (i.e. equation (2.15)), only now the variables are taken to have a slow x-dependence.

As plasma variables change on a scale (L), which is much larger than the wavelength, the approximation (2.24) would appear to be valid. However, at resonance the conductivity tensor changes on the scale of the absorption width (δ), which is often comparable in size to the wavelength (λ), and so WKB theory is not valid in this regime. We will consider it here though as firstly, it provides a simple and accurate description of the propagation of waves outside of the absorption region, and secondly, to compare its results with those from our full wave equations which will be derived in chapter three.

2.2.2 Full Wave Equations.

To give a complete description of a wave passing through a resonance we need then to use a full wave equation. For waves in the electron cyclotron range this will take the form of a differential equation and the simplest way of deriving this is to convert the wave vectors in the wave equations of WKB theory to differential operators, that is,

$$\mathbf{D}(\omega,k(x)) \rightarrow \mathbf{D}(\omega, -i\frac{d}{dx})\,, \qquad (2.25)$$

which amounts to an inverse Fourier transform. Doing this for the ordinary mode at the fundamental (i.e. taking (2.15) as our starting point.) gives,

$$\left(1 + \frac{1}{2}\frac{\omega_p^2}{\Omega^2} F_{7/2}\left(\frac{\mu x}{L}\right)\right)\frac{d^2E_{1z}}{dx^2} + \frac{\omega^2 - \omega_p^2}{c^2} E_{1z} = 0 . \qquad (2.26)$$

However, this equation, like others derived by this technique, does not conserve energy. The problem is that in making the transformation (2.25) we have ignored derivatives which may act on the conductivity tensor which, as we discussed earlier, may vary on the scale of the wavelength near resonance.

What is needed then, is a derivation of the full wave equation which will include such derivatives. As we are assuming that $\delta = L/\mu \sim \lambda$, we must expand according to,

$$k\rho \sim \frac{\mu\rho}{L} \sim \varepsilon , \qquad (2.27)$$

and, as this means changes to the conductivity tensor occur on a scale of the order of the wavelength, we may go further and conclude that $k \sim \frac{\omega}{c}$, which results in,

$$\varepsilon \sim k\rho \sim \frac{\omega}{c}\frac{v_t}{\Omega} \sim \frac{v_t}{c} . \qquad (2.28)$$

An analysis based on this ordering was first performed by Maroli et al (1986) and the equations they produced did indeed conserve energy. Their technique was, however, extremely complicated and applicable only to the simplest of problems. In chapter 3 we use a simpler technique to derive a full wave equation which is valid for propagation through all resonances in all wave modes. In chapter 4 we shall show how to expand this equation for a specific resonance or wave mode.

The technique is an extension of the work of Cairns et al (1991) into the relativistic regime. They used a derivation similar in form to that for a hot collisionless homogenous plasma (as in section 2.1.2), but included the gyrokinetic correction of Lashmore-Davies and Dendy (1989) in their calculation.

The gyrokinetic correction takes account of the fact that the electron's Larmor frequency should be calculated not at its position (x), but at its gyrocentre ($x + v_y/\Omega$). Denoting the frequency calculated at x as Ω_0, this would give,

$$\Omega = \Omega_0 - \frac{v_y}{L} . \tag{2.29}$$

The inclusion of this term has two effects upon our equations. Firstly, it introduces another source of resonance broadening, first described by Lashmore-Davies and Dendy (1989), known as gyrokinetic broadening. If we ignore relativistic and Doppler effects for a moment, then the resonance condition becomes,

$$\omega = n\,\Omega_0 + n\frac{v_y}{L}, \tag{2.30}$$

which gives a symmetric absorption profile on the scale of,

$$\frac{\delta\omega}{n\Omega} \sim \frac{\rho}{L}. \tag{2.31}$$

This is on a much smaller scale than either the relativistic broadening or the Doppler broadening and so in general can be ignored, a fact that will be discussed in more detail in chapter 4. Gyrokinetic broadening does play an important part in ion cyclotron resonance, where the Larmor radii (ρ) are larger, however. The second effect of the correction is to

include in the analysis derivatives that may act on the conductivity tensor which result in equations that are energy conserving and hence the desired self consistent analysis.

Returning to our three regimes of propagation, given by equations (2.18), (2.19) and (2.20), we see that in the case of oblique propagation, where by definition the absorption width is much greater than that for relativistic mass broadening, absorption occurs on a scale of many wavelengths. This means that derivatives acting on the conductivity tensor will be negligible, and so an analysis by the inverse Fourier transform method will suffice. However, in the other two cases (quasi-perpendicular propagation and the mixed case) absorption occurs on the scale of the wavelength and we must use the gyrokinetic correction in our analysis. This leaves us with the ordering,

$$k\rho \sim \frac{\mu\rho}{L} \sim N_z \sim \varepsilon . \qquad (2.32)$$

Our derivation then will include both the gyrokinetic correction and relativistic effects to give an energy conserving wave equation valid in the relativistic regime. Before this, however, we will first consider the practical question of the accessibility of resonances in a tokamak plasma.

2.3 Accessibility.

In the course of this thesis we wish to describe the propagation of waves in three specific cases, namely,

(i) The ordinary wave through the fundamental resonance.

(ii) The extraordinary wave through the fundamental and upper-hybrid resonance.

(iii) The extraordinary wave through the second harmonic resonance.

These waves must be launched from either the inside (high field incidence) or the outside (low field incidence) of the tokamak, and we wish to analyse the accessibility of these resonances. For this purpose the cold plasma theory of section (2.1.1) is sufficient.

For the ordinary wave the condition for propagation is that the wave frequency is greater than the plasma frequency, which is greatest at the centre. So, for the wave to reach the fundamental resonance ($\omega = \Omega$) we require only that,

$$\omega_p < \Omega \,, \tag{2.33}$$

at the plasma centre.

The propagation condition for the extraordinary mode is more complicated and we shall use the CMA diagram (Fig (2.1)) to describe it. Propagation through the tokamak is represented by a curve which begins on the Y-axis (as the density is zero outside of the plasma) and moves to the right as the plasma density increases. As the wave propagates towards the centre of the plasma, the curve moves downwards for high field incidence and upwards for low field incidence.

In Fig (2.1) the top two arrows represent the trajectory of extraordinary waves launched towards the upper-hybrid resonance with low (LFI) and high field incidence (HFI) respectively. As the curve for high field incidence must pass through the

evanescent (shaded) region this wave cannot propagate and so the upper-hybrid resonance can only be reached from the low field side.

Extraordinary waves launched from the low and high field sides towards the second harmonic resonance are represented by the bottom two arrows. This time the resonance is accessible from either side but we have the restriction that cyclotron resonance ($\omega = 2\Omega$) must occur before the cutoff which imposes the condition,

$$\omega_p^2 < 2\Omega^2 , \tag{2.34}$$

at the plasma centre.

Oblique propagation will modify these conditions, but for near perpendicular propagation this will be only slight.

3. THE GENERAL WAVE EQUATION.

Having discussed the limitations of WKB theory we shall now derive the general wave equation for high frequency ($\omega \sim \Omega_e$) waves in a relativistic plasma in the presence of an inhomogeneous magnetic field (McDonald et al (1994)). The solution of this wave equation is however extremely difficult and time consuming even by numerical methods. To enable a solution a technique will be indicated for its expansion and simplification.

3.1 Outline of the Model.

We shall consider a hot collisionless isotropic plasma in the presence of a magnetic field $\mathbf{B_0}$ which has a gradient in a perpendicular direction. Co-ordinates will be chosen so that the magnetic field lies in the z-direction and the gradient in the x-direction, with the field given by,

$$\mathbf{B_0} = B_0(0)\,(1 - x/L)\,\mathbf{e_z}\,. \tag{3.1}$$

Clearly, the magnetic field varies on a length scale L and other basic plasma parameters, such as temperature (T) and density (n_0), are taken to vary on the same scale.

We consider the propagation of plasma waves, in the x-z plane, which are harmonic in time (i.e. first order terms go as $e^{-i\omega t}$), giving the first order Maxwell's equation as,

$$-\nabla\times\nabla\times\mathbf{E_1} + i\omega\mu_0\,\mathbf{J_1} + \frac{\omega^2}{c^2}\,\mathbf{E_1} = \mathbf{0}\,, \tag{3.2}$$

which must be solved simultaneously with the equation of state. For a hot relativistic collisionless plasma this is the Vlasov equation,

$$\frac{\partial f}{\partial t} + \frac{1}{\gamma}\mathbf{u} \bullet \frac{\partial f}{\partial \mathbf{r}} + \frac{q}{m_0}\left(\mathbf{E} + \frac{1}{\gamma}\mathbf{u} \times \mathbf{B} \right) \bullet \frac{\partial f}{\partial \mathbf{u}} = 0 . \tag{3.3}$$

Linearised this becomes,

$$\frac{d^{(0)} f_1}{dt} = -\frac{q}{m_0}\left(\mathbf{E_1} + \frac{1}{\gamma}\mathbf{u} \times \mathbf{B_1} \right) \bullet \frac{\partial f_0}{\partial \mathbf{u}} , \tag{3.4}$$

where differentiation is performed along the equilibrium orbits.

3.2 Derivation of the Wave Equation.

The problem is then, to solve Maxwell's equations (3.2) and the linearised Vlasov equation (3.4) self consistently, but this time remembering that the magnetic field ($\mathbf{B_0}$) varies across the electron's Larmor radius. As we are assuming an isotropic plasma the second term on the right hand side vanishes.

We solve (3.4) for f_1 by the method of characteristics, to give,

$$f_1 = -\frac{q}{m_0} \int_{-\infty}^{t} dt' \, \mathbf{E_1}(\mathbf{r}',t') \bullet \frac{\partial f_0(t',\mathbf{r}',\mathbf{u}')}{\partial \mathbf{u}'} . \tag{3.5}$$

The prime denotes that the integration is carried out around the unperturbed orbits which are given, to dominant order, by,

$$x' = x + \frac{u_\perp}{\Omega}\left[\sin\left(\Omega\tau/\gamma - \theta\right) + \sin\theta\right] \tag{3.6a}$$

$$y' = y + \frac{u_\perp}{\Omega}\left[\cos\left(\Omega\tau/\gamma - \theta\right) - \cos\theta\right] + \frac{u_\perp^2\tau}{2\gamma\Omega L} \tag{3.6b}$$

$$z' = z + u_z\tau/\gamma \tag{3.6c}$$

$$t' = t + \tau \tag{3.6d}$$

$$u_x' = u_\perp \cos\left(\Omega\tau/\gamma - \theta\right) \tag{3.6e}$$

$$u_y' = -u_\perp \sin\left(\Omega\tau/\gamma - \theta\right) + \frac{u_\perp^2}{2\gamma\Omega L} \tag{3.6f}$$

$$u_z' = u_z \tag{3.6g}$$

where $(u_\perp,\theta,u_z)$ denotes the electron velocity in cylindrical co-ordinates and Ω denotes the Larmor frequency of the electron.

The perturbed current density is calculated from f_1 by,

$$\mathbf{J_1} = \int d^3\mathbf{u}\, q \frac{\mathbf{u}}{\gamma} f_1 \tag{3.7}$$

giving,

$$\mathbf{J_1} = -\frac{q^2}{m_0}\int d^3\mathbf{u}\,\frac{\mathbf{u}}{\gamma}\int_{-\infty}^{t} dt'\,\mathbf{E_1}(\mathbf{r}',t')\bullet\frac{\partial f_0(t',\mathbf{r}',\mathbf{u}')}{\partial \mathbf{u}'}. \tag{3.8}$$

If we express the perturbed current density, $\mathbf{E_1}$, in terms of a Fourier integral,

$$\mathbf{E_1}(\mathbf{r},t) = \int dk_x\,\mathbf{E_1}(k_x)\exp(i\mathbf{k}\bullet\mathbf{x} - i\omega t) \tag{3.9}$$

where $\mathbf{k} = (k_x,0,k_z)$, then the expression for the perturbed current density becomes,

$$\mathbf{J_1} = \int dk_x\,\Sigma(k_x,x)\bullet\mathbf{E_1}(k_x)\exp(i\mathbf{k}\bullet\mathbf{x} - i\omega t) \tag{3.10}$$

where,

$$\Sigma = -\frac{q^2}{m_0}\int d^3\mathbf{u}\int_{-\infty}^{0} d\tau\,\frac{\mathbf{u}}{\gamma}\frac{\partial f_0'}{\partial \mathbf{u}'}\exp\left(i\frac{k_x u_\perp}{\Omega}[\sin(\Omega\tau/\gamma-\theta)+\sin\theta] + ik_z u_z\tau/\gamma - i\omega\tau\right) \tag{3.11}$$

or using equations (3.6) to express $\partial f_0'/\partial \mathbf{u}'$ in terms of cylindrical co-ordinates,

$$\Sigma = -\frac{q^2}{m_0}\int d^3\mathbf{u}\int_{-\infty}^{0} d\tau\,\frac{\mathbf{u}}{\gamma}\left(\frac{\partial f_0}{\partial u_\perp}\cos(\theta-\Omega\tau/\gamma), \frac{\partial f_0}{\partial u_\perp}\sin(\theta-\Omega\tau/\gamma), \frac{\partial f_0}{\partial u_z}\right)$$

$$\times\exp\left(i\frac{k_x u_\perp}{\Omega}[\sin(\Omega\tau/\gamma-\theta)+\sin\theta] + ik_z u_z\tau/\gamma - i\omega\tau\right). \tag{3.12}$$

We now make use of the identity,

$$e^{ib\sin\phi} = \sum_{m=-\infty}^{\infty} J_m(b)\, e^{im\phi}\,, \tag{3.13}$$

which enables us to express the conductivity tensor as,

$$\Sigma = \sum_{n=-\infty}^{\infty} \Sigma_n$$

where,

$$\Sigma_n = -\frac{q^2}{m_0}\int d^3\mathbf{u} \int_{-\infty}^{0} d\tau \frac{\mathbf{u}}{\gamma}\left(\frac{\partial f_0}{\partial u_\perp}\frac{n\Omega}{k_x u_\perp} J_n\left(\frac{k_x u_\perp}{\Omega}\right), \frac{\partial f_0}{\partial u_\perp} i\, J_n'\left(\frac{k_x u_\perp}{\Omega}\right), \frac{\partial f_0}{\partial u_z} J_n\left(\frac{k_x u_\perp}{\Omega}\right)\right)$$

$$\times \exp\left(i\frac{k_x u_\perp}{\Omega}\sin\theta - in\theta\right)\exp\left(-\frac{i\tau}{\gamma}(\omega\gamma - k_z u_z - n\Omega)\right) \tag{3.14}$$

It is at this point that we include the gyrokinetic correction.

As discussed earlier the Larmor frequency of the electrons should be calculated, not at their position (x), but at their gyrocentres ($x+u_\perp\sin\theta/\Omega_0$). Generally, the effect can be ignored and we may take $\Omega = \Omega_0$, but in the rapidly varying resonant part of the τ integral the effect becomes important. Here we must take,

$$\Omega = \Omega_0(x+u_\perp\sin\theta/\Omega_0) = \Omega_0 - \frac{u_\perp}{L}\sin\theta\,, \tag{3.15}$$

giving,

$$\omega\gamma - k_z u_z - n\Omega = (\omega - n\Omega_0) - k_z u_z + \frac{\omega}{\mu}\frac{u^2}{u_t^2} + \frac{n u_\perp}{L}\sin\theta$$

$$= \frac{\omega}{\mu}\left(\xi_n - 2\alpha\frac{u_z}{u_t} + \frac{u^2}{u_t^2} + \frac{h_n u_\perp}{\Omega_0}\sin\theta\right), \qquad (3.16)$$

where, $\xi_n = \mu\dfrac{\omega - n\Omega_0}{\omega}$, $\alpha = N_z\dfrac{c}{u_t}$, $h_n = \dfrac{n\Omega_0\mu}{\omega L}$,

$$\mu = \frac{2c^2}{u_t^2}$$

and u_t is the mean square thermal speed defined by $u_t=\sqrt{2T_e/m_0}$. It should also be noted here that ξ_n is a spatially dependent quantity. Inserting this expression into the resonant term in (3.14) and changing the variable of integration in the second integral to t = $-\omega\tau/\mu\gamma$, we have,

$$\Sigma_n = -\frac{q^2}{m_0}\frac{\mu}{\omega}\int_0^\infty dt\,\exp(i\xi_n t)\int d^3\mathbf{u}\,\mathbf{u}$$

$$\times\left(\frac{\partial f_0}{\partial u_\perp}\frac{n\Omega_0}{k_x u_\perp}J_n\left(\frac{k_x u_\perp}{\Omega_0}\right), \frac{\partial f_0}{\partial u_\perp} i J_n'\left(\frac{k_x u_\perp}{\Omega_0}\right), \frac{\partial f_0}{\partial u_z}J_n\left(\frac{k_x u_\perp}{\Omega_0}\right)\right)$$

$$\times\exp\left(i\,(k_x+h_n t)\frac{u_\perp}{\Omega_0}\sin\theta - in\theta\right)\exp\left(-2i\alpha\frac{u_z}{u_t}t + i\frac{u^2}{u_t^2}t\right). \qquad (3.17)$$

As we are considering the weakly relativistic regime we assume a non-relativistic Maxwellian initial distribution function,

$$f_0 = n_0 \pi^{-3/2} u_t^{-3} \exp(-u^2/u_t^2) . \tag{3.18}$$

Using this and reapplying the identity (3.13) gives,

$$\Sigma_n = \frac{n_0 q^2}{m_0} \frac{\mu}{\omega} \int_0^\infty dt \exp(i\xi_n t) \int d^3\mathbf{u}\, 2\pi^{-3/2} u_t^{-5} \exp\left(- 2i\alpha t \frac{u_z}{u_t} - (1 - it) \frac{u^2}{u_t^2} \right)$$

$$\times \begin{bmatrix} \frac{(n\Omega_0)^2}{k_x (k_x+h_n t)} J_n J_n & iu_\perp \frac{n\Omega_0}{k_x+h_n t} J_n' J_n & u_z \frac{n\Omega_0}{k_x+h_n t} J_n J_n \\ - iu_\perp \frac{n\Omega_0}{k_x} J_n J_n' & u_\perp^2 J_n' J_n' & - iu_\perp u_z J_n J_n' \\ u_z \frac{n\Omega_0}{k_x} J_n J_n & iu_\perp u_z J_n' J_n & u_z^2 J_n J_n \end{bmatrix} . \tag{3.19}$$

The Bessel functions have arguments $k_x u_\perp/\Omega_0$ and $(k_x+h_n t)u_\perp/\Omega_0$ respectively. The velocity integral can be simplified further by taking the quadratic exponent and completing the square with the substitution

$$\mathbf{U} = \frac{\mathbf{u}}{u_t} (1-it)^{1/2} + \frac{i\alpha t}{(1-it)^{1/2}} \mathbf{e}_z, \tag{3.20}$$

to give,

$$\Sigma_n = \frac{n_0 q^2}{m_0}\frac{\mu}{\omega}\int_0^\infty dt \frac{\exp\left(i\xi_n t - \frac{\alpha^2 t^2}{1-it}\right)}{(1-it)^{5/2}} \int d^3\mathbf{U}\, 2\pi^{-3/2} \exp\left(-U^2\right)$$

$$\times \begin{bmatrix} \frac{n^2(1-it)}{k_x(k_x+h_n t)\rho^2} J_n J_n & iu_\perp \frac{n(1-it)^{1/2}}{(k_x+h_n t)\rho} J_n' J_n & -\frac{i\alpha n t}{(k_x+h_n t)\rho} J_n J_n \\ -iu_\perp \frac{n(1-it)^{1/2}}{k_x \rho} J_n J_n' & u_\perp^2 J_n' J_n' & -\frac{\alpha t}{(1-it)^{1/2}} u_\perp J_n J_n' \\ -\frac{i\alpha n t}{k_x \rho} J_n J_n & \frac{\alpha t}{(1-it)^{1/2}} u_\perp J_n' J_n & (u_z^2 - \frac{\alpha^2 t^2}{1-it}) J_n J_n \end{bmatrix}.$$

(3.21)

where $k_x\rho U_\perp(1-it)^{-1/2}$ and $(k_x+h_n t)\rho U_\perp(1-it)^{-1/2}$ are now the arguments of the Bessel functions. The θ and u_z integrals can now be performed trivially to give,

$$\Sigma_n = \frac{n_0 q^2}{m_0}\frac{\mu}{\omega}\int_0^\infty dt \frac{\exp\left(i\xi_n t - \frac{\alpha^2 t^2}{1-it}\right)}{(1-it)^{5/2}} \int_0^\infty dU_\perp\, 4\, U_\perp \exp\left(-U_\perp^2\right)$$

$$\times \begin{bmatrix} \frac{n^2(1-it)}{k_x(k_x+h_n t)\rho^2} J_n J_n & iU_\perp \frac{n(1-it)^{1/2}}{(k_x+h_n t)\rho} J_n' J_n & -\frac{i\alpha n t}{(k_x+h_n t)\rho} J_n J_n \\ -iU_\perp \frac{n(1-it)^{1/2}}{k_x \rho} J_n J_n' & U_\perp^2 J_n' J_n' & -\frac{\alpha t}{(1-it)^{1/2}} U_\perp J_n J_n' \\ -\frac{i\alpha n t}{k_x \rho} J_n J_n & \frac{\alpha t}{(1-it)^{1/2}} U_\perp J_n' J_n & (\frac{1}{2} - \frac{\alpha^2 t^2}{1-it}) J_n J_n \end{bmatrix}.$$

(3.22)

Thus, the required term in Maxwell's equation can be expressed as,

$$i\omega\mu_0 \mathbf{J_1}(x) = i\mu \frac{\omega_p^2}{c^2} \sum_{n=-\infty}^{\infty} \int dk_x \exp(ik_x x) \int_0^{\infty} dt \frac{\exp\left(i\xi_n t - \frac{a_n t^2}{1 - it}\right)}{(1 - it)^{5/2}} \mathbf{C_n}(k_x, t) \bullet \mathbf{E_1}(k_x) \tag{3.23}$$

where,

$$\mathbf{C_n} = e^{-\lambda} \times$$

$$\begin{bmatrix} \frac{n^2}{\lambda} I_n & in\left(I_n' - \frac{k_x}{k_x + h_n t} I_n\right) & -\frac{2i\alpha nt}{(k_x + h_n t)\rho} I_n \\ -in\left(I_n' - \frac{k_x + h_n t}{k_x} I_n\right) & \left(2\lambda + \frac{n^2}{\lambda}\right) I_n - \left(2\lambda + \frac{(h_n t\rho)^2}{2(1 - it)}\right) I_n' & -\frac{\alpha\rho t}{1 - it}\left(k_x I_n' - (k_x + h_n t) I_n\right) \\ -\frac{2i\alpha nt}{k_x \rho} I_n & \frac{\alpha\rho t}{1 - it}\left((k_x + h_n t) I_n' - k_x I_n\right) & \left(1 - \frac{2\alpha^2 t^2}{1 - it}\right) I_n \end{bmatrix}$$

and

$$\lambda = \frac{\frac{1}{2} k_x (k_x + h_n t)\rho^2}{1 - it}, \qquad \xi_n = \mu \frac{\omega - n\Omega_0}{\omega}, \qquad h_n = \frac{n\Omega_0 \mu}{\omega L},$$

$$a_n = \alpha^2 + \left(\frac{h_n \rho}{2}\right)^2, \qquad \alpha = N_z \frac{c}{u_t}, \qquad \mu = \frac{2c^2}{u_t^2}, \qquad \rho = \frac{u_t}{\Omega_0}, \qquad \omega_p^2 = \frac{n_0 q^2}{\varepsilon_0 m_0},$$

and the modified Bessel functions all have argument λ.

Equation (3.23) gives us an expression for the response of the plasma which when inserted into Maxwell's equations (3.2) gives us a complete integro-differential equation

describing high frequency wave propagation in a weakly relativistic plasma in the presence of an inhomogeneous magnetic field. However, the equation is too complicated in this form to be solved even numerically.

Firstly, the equation contains an infinite summation, over n, which represents the different harmonics in the response of the plasma. For non-resonant terms thermal effects are not important and we may approximate such terms by their cold plasma response. As the separation of the resonances is given by $\Delta_n = L/n$ and the width of these resonances is given by $\delta = L/\mu$, then provided $\mu > n$, which as $\mu >> 1$ will be the case for the significant lower harmonic resonances, the resonances do not overlap. This means we need only deal with one resonance (n_r) and keep only the $n=n_r$ term in the summation in (3.23), replacing all others by their cold plasma ($k_x \rho \rightarrow 0$) approximation.

More importantly, we can reduce the equation to a simple linear ordinary differential equation by expanding $\mathbf{C_n}$ into a polynomial in k_x and t. This can be done by using the ordering (2.30). When such a polynomial is inserted back into (3.23) the result is a differential expression for the response of the plasma which when substituted back into (3.2) gives a differential wave equation.

4. DERIVATION OF THE DIFFERENTIAL WAVE EQUATIONS.

As discussed before the general wave equation, derived in chapter two, is too complicated to solve in itself and so instead we expand it into a differential equation.

4.1 The General Technique.

For a given resonance we may take the cold plasma contribution from the non-resonant part of the dielectric tensor together with higher order terms from the resonant part. The expansion is ordered in terms of the small parameter ε, discussed in chapter 2.

The procedure is to take our general wave equation (3.23) and expand the matrix $\mathbf{C_n}(k_x,t)$ using the ordering,

$$k_x\rho \sim \varepsilon\,, \qquad h_n\rho t \sim \varepsilon \qquad \text{and} \qquad \alpha \sim 1 \tag{4.1}$$

(see section 2.2.2). Doing this results in a polynomial in k_x and t, and we can produce a differential equation for the perturbed current density (J_1) from this by noting the relation,

$$\int dk_x\, E_1(k_x) \exp(i\mathbf{k}\bullet\mathbf{x} - i\omega t) \int_0^\infty dt \frac{\exp\left[i\xi_n t - \frac{a_n t^2}{(1 - it)}\right]}{(1 - it)^{5/2}} \left\{ \frac{(ik_x)^j\,(it)^m}{(1-it)^p} \right\}$$

$$= i \frac{d^j E_1}{dx^j}\, \mathfrak{F}_{p+5/2,\,m}\left(\xi_n\,,\, a_n\right) \tag{4.2}$$

where the $\mathfrak{F}$'s are the relativistic plasma dispersion functions (RPDF's), developed by Dnestrovskii et al (1964) and Shkarofsky (1966). The definitions of these functions, along with some important relations, are given in the appendix.

In effect the RPDF's represent a resonance that is broadened by relativistic mass increase as well as by other processes, associated with the second argument (a_n), which are linearly dependent on velocity. From (3.23) we see that the second argument is given by,

$$a_n = \alpha^2 + \left(\frac{h_n \rho}{2}\right)^2, \tag{4.3}$$

which has two components. The first ($\alpha^2 = \frac{1}{2} \mu N_z^2$) is due to the Doppler broadening and the second ($\frac{1}{4} h_n^2 \rho^2$) is due to the gyrokinetic broadening. As we discussed in chapter 2, the gyrokinetic broadening is usually negligible compared with relativistic or Doppler broadening. Here we see that the second term is of order ε^2 and so can in fact be ignored (i.e. $a_n = \alpha^2$).

Derivatives acting on the RPDF's can be expressed in terms of spatial derivatives by noting that to leading order,

$$(h_n)^m \mathfrak{F}_{q,m}\left(\xi_n, \tfrac{1}{2}\mu N_z^2\right) = (h_n)^m \frac{\partial^m \mathfrak{F}_q}{\partial \xi^m} \sim \frac{d^m \mathfrak{F}_q}{dx^m}. \tag{4.4}$$

Once derived in this fashion, the expression for the perturbed current density can be used to produce a differential wave equation by inserting into Maxwell's equations (3.2) which, with the ordering of (4.1) become,

$$i\omega\mu_0 J_{1x} + \frac{\omega^2}{c^2} E_{1x} = 0, \tag{4.5}$$

$$\frac{d^2 E_{1y}}{dx^2} + i\omega\mu_0 J_{1y} + \frac{\omega^2}{c^2} E_{1y} = 0, \tag{4.6}$$

$$\frac{d^2E_{1z}}{dx^2} + i\omega\mu_0 J_{1z} + \frac{\omega^2}{c^2}E_{1z} = 0\,, \tag{4.7}$$

as derivatives with respect to z are of relative order $N_z \sim \varepsilon$.

4.1.1 Cold plasma terms.

As we have said, the non-resonant components of the perturbed current density may be represented by their cold plasma approximations. From the cold plasma theory of section 2.1.1. we see that the expressions for the perturbed current densities are,

$$i\omega\mu_0 J_{1x} = -\frac{\omega_p^2}{c^2}\frac{\omega^2}{\omega^2 - \Omega^2}E_{1x} - i\frac{\omega_p^2}{c^2}\frac{\omega\,\Omega}{\omega^2 - \Omega^2}E_{1y}\,, \tag{4.8}$$

$$i\omega\mu_0 J_{1y} = i\frac{\omega_p^2}{c^2}\frac{\omega\,\Omega}{\omega^2 - \Omega^2}E_{1x} - \frac{\omega_p^2}{c^2}\frac{\omega^2}{\omega^2 - \Omega^2}E_{1y}\,, \tag{4.9}$$

$$i\omega\mu_0 J_{1z} = -\frac{\omega_p^2}{c^2}E_{1z}\,. \tag{4.10}$$

We shall now derive the full wave equations for several specific cases. We shall pay special attention to the perpendicular O-mode at the fundamental as it is the simplest case and consequently has been dealt with by many other authors enabling us to make comparisons between our results and theirs.

4.2 Perpendicular Propagation.

At perpendicular incidence the wave equation decouples into an equation for the perpendicular field (E_{1x},E_{1y}), representing the extraordinary mode, and an equation for the parallel field (E_{1z}), representing the ordinary mode.

4.2.1 The O-mode at the fundamental resonance.

To describe the O-mode we need only consider the zz element of the plasma response. Following the general procedure outlined in 4.1, we begin by writing down the general expression for $\mathbf{C_n}$, which in this case only involves C_{zzn} ,given by,

$$C_{zzn} = e^{-\lambda} I_n \,. \tag{4.11}$$

For the fundamental we require the n=1 term, which expanded to $O(\varepsilon^2)$ is,

$$C_{zz1} \sim \frac{\lambda}{2} = \frac{\rho^2}{4} \frac{k_x^2 + k_x h_1 t}{1 - it} \,. \tag{4.12}$$

We then insert this back into our general wave equation (3.23) and solve, using the identity (4.2). Combined with the cold plasma term (4.10) this gives us the following expression for the perturbed current density,

$$i\omega\mu_0 J_{1z} = \frac{\omega_p^2}{c^2} \frac{\mu\rho^2}{4} F_{7/2}(\xi_1) \frac{d^2E_{1z}}{dx^2} + \frac{\omega_p^2}{c^2} \frac{\mu\rho^2 h_1}{4} F'_{7/2}(\xi_1) \frac{dE_{1z}}{dx} - \frac{\omega_p^2}{c^2} E_{1z} \,. \tag{4.13}$$

This is then inserted into Maxwell's equation (4.7) to give, after noting the identity (4.3),

$$\frac{d}{dx}\left\{\left[1+\frac{1}{2}\frac{\omega_p^2}{\Omega_0^2}F_{7/2}\left(\mu\frac{\omega-\Omega_0}{\omega}\right)\right]\frac{dE_{1z}}{dx}\right\}+\left(\frac{\omega^2-\omega_p^2}{c^2}\right)E_{1z}=0\,, \qquad (4.14)$$

the full wave equation for the O-mode propagating perpendicularly through the fundamental resonance. This is exactly the equation derived by Maroli et al (1986).

Comparing with the equation produced by the inverse Fourier transform method (2.26) we see that we now have an extra term consisting of a derivative of the RPDF. In fact all equations produced by this method differ from those produced by the inverse Fourier transform method by terms which consist of derivatives acting on the equilibrium distribution functions and these terms are the very ones necessary for energy conservation which we shall discuss in greater detail in chapter 5. It is interesting to note that despite the lack of energy conservation in (2.26) the equation does still give the correct values for the transmission, reflection and absorption coefficients. This is because the spatial derivative of any solution of (4.14) is a solution of (2.26).

To gain some analytical insight into the properties of our equation (4.14) we can attempt a WKB solution. This amounts to solving the equation,

$$-\left(1+\frac{1}{2}\frac{\omega_p^2}{\Omega_0^2}F_{7/2}\right)k_x^2+\frac{1}{2}\frac{\omega_p^2}{\Omega_0^2}\frac{dF_{7/2}}{dx}ik_x+\frac{\omega^2-\omega_p^2}{c^2}=0\,, \qquad (4.15)$$

where, if we choose the resonance to lie at x=0, the RPDF's have argument $\xi_1 = \mu x/L$. To pre-empt any confusion, we should contrast the WKB solution of our full wave equation (given by equation (4.15)), which includes the gyrokinetic correction, with the standard WKB equation (2.15). Assuming the absorption is weak we may expand k_x as $k_0 + \delta k$, where k_0 is the cold plasma solution ($k_0^2c^2 = \omega^2 - \omega_p^2$, see equation (2.5)). This gives the imaginary part of δk as,

$$\delta k_I = -\frac{1}{4}\frac{\omega_p^2}{\Omega_0^2} k_0 \left[\mathrm{Im}\,(F_{7/2}) - \frac{\mu}{k_0 L}\,\mathrm{Re}\,(F'_{7/2}) \right]. \qquad (4.16)$$

The first part of this expression is the standard term we would get by the WKB method, whereas the second term is due to the gyrokinetic correction. Its relevance is dependent on the factor μ/k_0L which is essentially the ratio of the wavelength to the absorption width. If we look now at the optical depth then we see that, as the second term in δk_I is a spatial derivative of a function that tends to zero either side of the resonance (A.17) and so will integrate across the plasma to zero, only the first term will contribute, giving,

$$\tau = 2 \int_{-\infty}^{\infty} dx\, \delta k_I = \frac{\pi}{2}\frac{\omega_p^2}{\Omega_0^2}\frac{k_0 L}{\mu}, \qquad (4.17)$$

where we have used the identity (A.18) for the imaginary part of the Dnestrovskii function. This then is the same value for the optical depth that we would obtain without the gyrokinetic correction. However, if we look at the absorption profiles from (4.16) (Figures (4.1a) and (4.1b), for high field incidence ($k_0 > 0$) and low field incidence ($k_0 < 0$) respectively) we see that the second term has made a significant contribution. In both cases the dotted line represents the standard result and the solid line the new profile. For high field incidence the peak absorption is now stronger and, to compensate this, we have a region of emission, energy passing from the plasma to the wave, which extends below the resonance ($\Omega<\omega$). This local emission is not due to energy actually being lost by the plasma, but is instead identified as the excess of energy absorbed around the absorption peak redistributed by a kinetic energy flux in the plasma. The second term in equation (4.16) then, represents this kinetic energy flux. For low field incidence the gyrokinetic correction has the reverse effect, with excess energy being absorbed below the resonance

and flowing to the peak, reducing the nett absorption there. In chapter 5 we shall perform a more exact full wave calculation of energy flows.

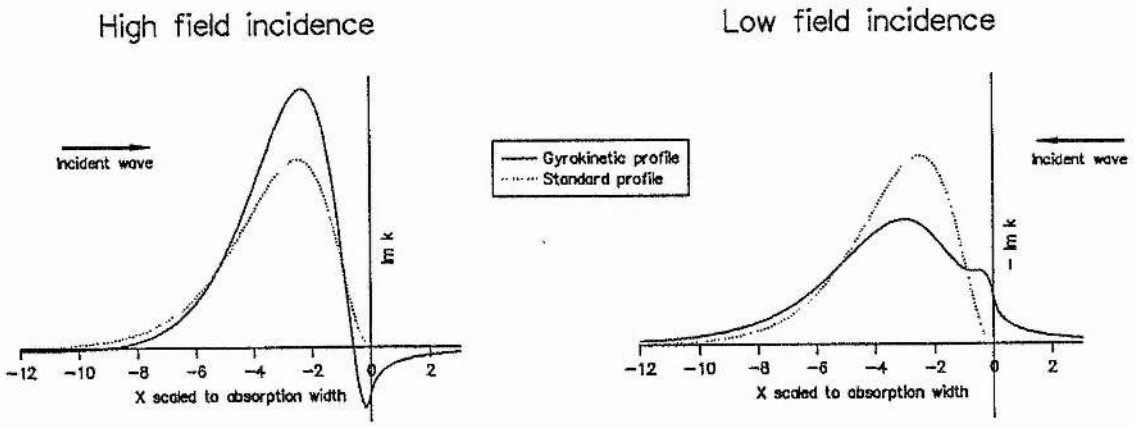

Figures 4.1a and 4.1b

WKB absorption profiles for $\mu/k_0L = 0.7$

Finally, we wish to compare our result (4.14) with the earlier work of Cairns et al (1991) which, as discussed earlier, included the gyrokinetic correction but did not account for relativistic effects. As here, they derived an equation for the O-mode propagating perpendicularly through the fundamental which had an absorption profile due to gyrokinetic broadening. To reproduce this we must consider a regime in which gyrokinetic broadening is dominant and so can not be ignored in our expression for the RPDF. This will mean that in (4.14) the Dnestrovskii function should be replaced by the generalised Dnestrovskii function $\mathfrak{F}(\xi_1, \frac{1}{4} h_1^2 \rho^2)$. For gyrokinetic absorption to dominate the second argument must be much greater than one in the resonance region, which amounts to the condition,

$$\frac{1}{4} h_1^2 \rho^2 = \left(\frac{\mu\rho}{2L}\right)^2 >> 1 . \qquad (4.18)$$

If this condition is satisfied then if we take the resonance to lie at x=0 (that is, we take $\Omega_0 = \omega(1 - x/L)$ as our expression for the cyclotron frequency) and note the relation (A.18), our wave equation becomes,

$$\frac{d}{dx}\left\{\left[\, 1 + \frac{\rho L}{4}\frac{\omega_p^2}{c^2} Z(x/\rho) \,\right]\frac{dE_{1z}}{dx}\right\} + \left(\frac{\omega^2 - \omega_p^2}{c^2}\right)E_{1z} = 0\,, \qquad (4.19)$$

the equation produced by Cairns et al (1991). However, according to our ordering (4.1), the second argument $\frac{1}{4} h_1^2 \rho^2 \sim \varepsilon^2$, which reflects the fact that the condition (4.18) is almost never satisfied in any physical situation.

4.2.2 The O-mode at the fundamental resonance with $k_y \neq 0$.

Our derivation of the general wave equation (3.23) did not consider propagation in the y-direction. There was no theoretical reason for this, the theory is perfectly capable of accommodating such propagation. However its inclusion results in a further summation over Bessel functions and so its omission was made to enable us to illustrate the theory whilst keeping the algebra as simple as possible.

In chapter 7, however, we illustrate how the theory can be extended to further geometries and, as an example, derive the wave equation for the ordinary mode propagating through the fundamental perpendicularly to the magnetic field but obliquely to the gradient. As we shall be solving this numerically in chapter 6, we shall include it here for completeness.

$$\frac{d}{dx}\left\{\left[\,1+\frac{1}{2}\frac{\omega_p^2}{\Omega_0^2}F_{7/2}\,\right]\frac{dE_{1z}}{dx}\right\}$$

$$+\left(-k_y^2+\frac{1}{2}\frac{\omega_p^2}{\Omega_0^2}\left[-k_y^2F_{7/2}+k_y\frac{dF_{7/2}}{dx}\right]+\frac{\omega^2-\omega_p^2}{c^2}\right)E_{1z}=0\,, \tag{4.20}$$

where the relativistic plasma distribution functions all have $\mu\,(1-\Omega_0/\omega)$ as their argument. Clearly, in the limit $k_y \rightarrow 0$ this equation does tend to (4.14) the equation for propagation purely in the x-direction.

4.2.3 The X-mode at the first harmonic resonance.

The calculation for the X-mode at the fundamental and, nearby, first harmonic resonances requires the derivation of the xx, xy, yx and yy elements. To second order in ε the C_1 matrix elements are,

$$C_{xx1} \sim \frac{1}{2}-\frac{\rho^2}{4}\frac{k_x^2+k_xh_1t}{1-it}, \tag{4.21}$$

$$C_{xy1} \sim \frac{1}{2}i-\frac{i\rho^2}{4}\frac{2k_x^2+k_xh_1t}{1-it}, \tag{4.22}$$

$$C_{yx1} \sim -\frac{1}{2}i+\frac{i\rho^2}{4}\frac{2k_x^2+3k_xh_1t+h_1^2t^2}{1-it}, \tag{4.23}$$

$$C_{yy1} \sim \frac{1}{2}-\frac{\rho^2}{4}\frac{3k_x^2+3k_xh_1t+h_1^2t^2}{1-it}. \tag{4.24}$$

which we combine with the n= -1 elements (which differ only by a sign, calculated by noting the positions of the n's in (3.23) along with the identity $h_{-1} = -h_1$) to give a full expression for the perturbed current density. When combined with Maxwell's equations (Equations (4.5) and (4.6)) we have the full wave equations,

$$-\mu\frac{\omega_p^2}{c^2}\left(\frac{\rho^2}{4}F_{7/2}(S)\frac{d^2E_{1x}}{dx^2}+\frac{\rho^2h_1}{4}F'_{7/2}(A)\frac{dE_{1x}}{dx}+\frac{1}{2}F_{5/2}(S)\,E_{1x}\right.$$

$$\left.+\,i\frac{\rho^2}{2}F_{7/2}(A)\frac{d^2E_{1y}}{dx^2}+i\frac{\rho^2h_1}{4}F'_{7/2}(S)\frac{dE_{1y}}{dx}+\frac{1}{2}i\,F_{5/2}(A)\,E_{1y}\right)$$

$$+\frac{\omega^2}{c^2}E_{1x}=0, \qquad (4.25)$$

$$\frac{d^2E_{1y}}{dx^2}-\mu\frac{\omega_p^2}{c^2}\left(-i\frac{\rho^2}{2}F_{7/2}(A)\frac{d^2E_{1x}}{dx^2}-i\frac{3\rho^2h_1}{4}F'_{7/2}(S)\frac{dE_{1x}}{dx}\right.$$

$$-i\left(\frac{1}{2}F_{5/2}(A)+\frac{\rho^2h_1^2}{4}F''_{7/2}(A)\right)E_{1x}+\frac{3\rho^2}{4}F_{7/2}(S)\frac{d^2E_{1y}}{dx^2}$$

$$\left.+\frac{3\rho^2h_1}{4}F'_{7/2}(A)\frac{dE_{1y}}{dx}+\left(\frac{1}{2}F_{5/2}(S)+\frac{\rho^2h_1^2}{4}F''_{7/2}(S)\right)E_{1y}\right)$$

$$+\frac{\omega^2}{c^2}E_{1y}=0, \qquad (4.26)$$

where $F_q(S) = F_q(\xi_1) + F_q(\xi_{-1})$ and $F_q(A) = F_q(\xi_1) - F_q(\xi_{-1})$. It should be noted here, that the cold plasma contribution to the perturbed current density is due to the n=1 and n= -1 harmonics and does not have to be included in our expressions explicitly.

4.2.4 The X-mode at the second harmonic resonance.

For the second harmonic resonance we must calculate the four elements of the **C** matrix for n=2. To second order, these elements are,

$$C_{xx2} \sim \frac{\rho^2}{4}\frac{k_x^2 + k_x h_2 t}{1 - it}, \tag{4.27}$$

$$C_{xy2} \sim \frac{i\rho^2}{4}\frac{k_x^2 + k_x h_2 t}{1 - it}, \tag{4.28}$$

$$C_{yx2} \sim -\frac{i\rho^2}{4}\frac{k_x^2 + k_x h_2 t}{1 - it}, \tag{4.29}$$

$$C_{yy2} \sim \frac{\rho^2}{4}\frac{k_x^2 + k_x h_2 t}{1 - it}, \tag{4.30}$$

which, when inserted in (3.23) and combined with the cold plasma terms (equations (4.8) and (4.9)) and Maxwell's equations (equations (4.5) and (4.6)), give the following system of wave equations,

$$-\mu\frac{\omega_p^2}{c^2}\left(-\frac{\rho^2}{4}F_{7/2}(\xi_2)\frac{d^2E_{1x}}{dx^2} - \frac{\rho^2 h_2}{4}F'_{7/2}(\xi_2)\frac{dE_{1x}}{dx} + \frac{1}{\mu}\frac{\omega^2}{\omega^2 - \Omega^2}E_{1x}\right.$$

$$\left.-\frac{i\rho^2}{4}F_{7/2}(\xi_2)\frac{d^2E_{1y}}{dx^2} - \frac{i\rho^2 h_2}{4}F'_{7/2}(\xi_2)\frac{dE_{1y}}{dx} + \frac{i}{\mu}\frac{\omega\,\Omega}{\omega^2 - \Omega^2}E_{1y}\right)$$

$$+\frac{\omega^2}{c^2}E_{1x} = 0, \tag{4.31}$$

$$\frac{d^2E_{1y}}{dx^2} - \mu\frac{\omega_p^2}{c^2}\left(\frac{i\rho^2}{4}F_{7/2}(\xi_2)\frac{d^2E_{1x}}{dx^2} + \frac{i\rho^2h_2}{4}F'_{7/2}(\xi_2)\frac{dE_{1x}}{dx} \right.$$

$$- \frac{i}{\mu}\frac{\omega\,\Omega}{\omega^2 - \Omega^2}E_{1x} - \frac{\rho^2}{4}F_{7/2}(\xi_2)\frac{d^2E_{1y}}{dx^2} - \frac{\rho^2h_2}{4}F'_{7/2}(\xi_2)\frac{dE_{1y}}{dx}$$

$$\left. + \frac{1}{\mu}\frac{\omega^2}{\omega^2 - \Omega^2}E_{1y} \right) + \frac{\omega^2}{c^2}E_{1y} = 0. \qquad (4.32)$$

4.3 Oblique Propagation.

Here, we must include the xz, yz, zx and zy elements, which are no longer non-zero, leaving us with a system of three second order differential equations which describe both the ordinary and extraordinary modes. Our RPDF's now become the full Shkarofsky functions, of the form $\mathfrak{F}_q(\xi_n, \frac{1}{2}\mu N_z^2)$, which describe both relativistic and Doppler broadening of the absorption profile.

4.3.1 The X-mode at the first harmonic resonance.

Expanding $\mathbf{C}_1$ and $\mathbf{C}_{-1}$ to second order, once more, we find that the xx, xy, yx and yy elements are the same as those given in equations (4.21), (4.22), (4.23) and (4.24). The other elements are,

$$C_{xz1} \sim \frac{i\alpha\rho}{2}\frac{k_x t}{1 - it}, \qquad (4.33)$$

$$C_{yz1} \sim -\frac{\alpha\rho}{2}\frac{k_x t}{1 - it}, \qquad (4.34)$$

$$C_{zx1} \sim -\frac{i\alpha\rho}{2}\frac{k_x t + h_1 t^2}{1 - it}, \qquad (4.35)$$

$$C_{zy1} \sim \frac{\alpha\rho}{2}\frac{k_x t + h_1 t^2}{1 - it}, \tag{4.36}$$

$$C_{zz1} \sim \frac{\rho^2}{4}\frac{k_x^2 + k_x h_1 t}{1 - it} - \frac{\alpha^2\rho^2}{2}\frac{k_x^2 t^2 + k_x h_1 t^3}{1 - it}. \tag{4.37}$$

The wave equation is then calculated, as before, by inserting these terms in our general wave equation (3.23), to calculate the perturbed current density, and then inserting this in Maxwell's equations (4.5), (4.6) and (4.7). The resulting system of wave equations is,

$$\begin{aligned} -\mu\frac{\omega_p^2}{c^2}\Bigg(& \frac{\rho^2}{4}\mathfrak{F}_{7/2}(S)\frac{d^2E_{1x}}{dx^2} + \frac{\rho^2 h_1}{4}\mathfrak{F}'_{7/2}(A)\frac{dE_{1x}}{dx} + \frac{1}{2}\mathfrak{F}_{5/2}(S)\,E_{1x} \\ & + i\frac{\rho^2}{2}\mathfrak{F}_{7/2}(A)\frac{d^2E_{1y}}{dx^2} + i\frac{\rho^2 h_1}{2}\mathfrak{F}'_{7/2}(S)\frac{dE_{1y}}{dx} + \frac{1}{2}i\,\mathfrak{F}_{5/2}(A)\,E_{1y} \\ & + \frac{i\alpha\rho}{2}\mathfrak{F}'_{7/2}(A)\frac{dE_{1z}}{dx}\Bigg) + \frac{\omega^2}{c^2}E_{1x} = 0, \end{aligned} \tag{4.38}$$

$$\begin{aligned} \frac{d^2E_{1y}}{dx^2} - \mu\frac{\omega_p^2}{c^2}\Bigg(& -i\frac{\rho^2}{2}\mathfrak{F}_{7/2}(A)\frac{d^2E_{1x}}{dx^2} - i\frac{3\rho^2 h_1}{4}\mathfrak{F}'_{7/2}(S)\frac{dE_{1x}}{dx} \\ & - i\left(\frac{1}{2}\mathfrak{F}_{5/2}(A) + \frac{\rho^2 h_1^2}{4}\mathfrak{F}''_{7/2}(A)\right)E_{1x} + \frac{3\rho^2}{4}\mathfrak{F}_{7/2}(S)\frac{d^2E_{1y}}{dx^2} \\ & + \frac{3\rho^2 h_1}{4}\mathfrak{F}'_{7/2}(A)\frac{dE_{1y}}{dx} + \left(\frac{1}{2}\mathfrak{F}_{5/2}(S) + \frac{\rho^2 h_1^2}{4}\mathfrak{F}''_{7/2}(S)\right)E_{1y} \\ & + \frac{\alpha\rho}{2}\mathfrak{F}'_{7/2}(S)\frac{dE_{1z}}{dx}\Bigg) + \frac{\omega^2}{c^2}E_{1y} = 0, \end{aligned} \tag{4.39}$$

$$\frac{d^2E_{1z}}{dx^2} - \mu\frac{\omega_p^2}{c^2}\left(\frac{i\alpha\rho}{2}\mathfrak{F}'_{7/2}(A)\frac{dE_{1x}}{dx} + \frac{i\alpha\rho h_1}{2}\mathfrak{F}''_{7/2}(S)E_{1x} - \frac{\alpha\rho}{2}\mathfrak{F}'_{7/2}(S)\frac{dE_{1y}}{dx}\right.$$

$$- \frac{\alpha\rho h_1}{2}\mathfrak{F}''_{7/2}(A)E_{1y} - \left(\frac{\rho^2}{4}\mathfrak{F}_{7/2}(S) + \frac{\alpha^2\rho^2}{4}\mathfrak{F}''_{7/2}(S)\right)\frac{d^2E_{1z}}{dx^2}$$

$$\left. - \left(\frac{\rho^2 h_1}{4}\mathfrak{F}'_{7/2}(A) + \frac{\alpha^2\rho^2 h_1}{4}\mathfrak{F}'''_{7/2}(A)\right)\frac{dE_{1z}}{dx} + \frac{1}{\mu}\right) + \frac{\omega^2}{c^2}E_{1z} = 0. \qquad (4.40)$$

where, $\mathfrak{F}_q(S) = \mathfrak{F}_q(\xi_1, \frac{1}{2}\mu N_z^2) + \mathfrak{F}_q(\xi_{-1}, \frac{1}{2}\mu N_z^2)$

and $\mathfrak{F}_q(A) = \mathfrak{F}_q(\xi_1, \frac{1}{2}\mu N_z^2) - \mathfrak{F}_q(\xi_{-1}, \frac{1}{2}\mu N_z^2)$.

5. ENERGY CONSERVATION.

Having derived the differential wave equations describing electromagnetic waves in a plasma at different resonances, we are now in a position to discuss more precisely what is meant by the analysis being self-consistent in terms of the equations conserving energy.

To do this we must derive the energy equation for the wave-plasma interaction, which is second order. This results in a considerable complication of the mathematics and so we shall deal here only with the simplest case that of the ordinary mode with perpendicular propagation through the fundamental resonance.

5.1 The Energy Equation.

The energy equation for a plasma is derived by taking the Vlasov equation (2.12), multiplying by the kinetic energy (T) and integrating over all velocities. The resulting equation is,

$$\mathbf{E} \bullet \mathbf{J} = P + \nabla \bullet \mathbf{S} , \qquad (5.1)$$

where,

$$P = \frac{\partial}{\partial t} \int d^3\mathbf{u} \; T \, f(\mathbf{r},\mathbf{u},t) , \qquad (5.2)$$

is the power absorbed by the plasma from the electromagnetic fields (clearly, if it is negative it represents power flowing from the plasma to the electromagnetic fields), and,

$$\mathbf{S} = \int d^3\mathbf{u} \; T \, \mathbf{v} \, f(\mathbf{r},\mathbf{u},t) , \qquad (5.3)$$

is the kinetic power flux (or sloshing flux), which represents kinetic power flowing around the plasma. If we integrate across the whole plasma the $\nabla \bullet \mathbf{S}$ term vanishes which represents the conservation of kinetic energy in the plasma.

To describe energy flow in a plasma wave (where terms are taken to go as $e^{-i\omega t}$), we must take the second order energy equation, averaged over time, which is,

$$\frac{1}{2}\mathrm{Re}\left(\mathbf{E}_1^* \bullet \mathbf{J}_1\right) = P + \nabla \bullet \mathbf{S}\,, \tag{5.4}$$

where P and **S** are now second order terms.

5.2 The O-Mode Propagating Perpendicularly through the Fundamental.

As discussed earlier, we shall now derive the energy equation for the O-Mode at the fundamental for perpendicular propagation. If we look at equation (5.4) term by term we see that, as we derived $\mathbf{J}_1$ in section 4.2.1 (equation (4.13)), the first term (the power flow from the wave to the plasma) can be trivially calculated. It remains then only to calculate the other two terms.

5.2.1 Power Absorption.

We begin by calculating the power absorbed by the plasma. To do this we must look at the second order Vlasov equation,

$$\frac{d^{(0)}f_2}{dt} = -\frac{q}{m}\left(\mathbf{E}_1 + \frac{1}{\gamma}\mathbf{v}\times\mathbf{B}_1\right) \bullet \frac{\partial f_1}{\partial \mathbf{u}} - \frac{q}{m}\left(\mathbf{E}_2 + \frac{1}{\gamma}\mathbf{v}\times\mathbf{B}_2\right) \bullet \frac{\partial f_0}{\partial \mathbf{u}}\,. \tag{5.5}$$

The first order terms are all harmonic in time - with frequency ω - and so the second order distribution function is, as pointed out by Maroli et al (1988), of the form

$$f_2(x,\mathbf{u},t) = g(x,\mathbf{u})\, t + h(x,\mathbf{u},t)\,, \tag{5.6}$$

where h is again harmonic in time with frequency 2ω.

The secular term, g, comes from the absorption of the wave energy by the plasma and the only non-zero contribution to it comes from the first term on the right hand side in (5.5) combined with the resonant component of f_1,

$$g = -\frac{q}{m}\frac{\Omega_0}{4\pi}\int_0^{2\pi/\Omega_0} d\tau\ \frac{1}{2}\,\mathrm{Re}\left(E^{*}_{1z}(x',t')\,\frac{\partial f_{1R}(x',\mathbf{u}',t')}{\partial u_z}\right). \tag{5.7}$$

By the analysis of chapter 3 we can express the resonant component of f_1 as,

$$f_{1R} = \int dk_x \int_0^{\infty} dt\ \mathbb{F}_R(k_x,t,\mathbf{u})\, E_{1z}(k_x)\exp(ik_x x + i\xi_1 t)\,, \tag{5.8}$$

where $\xi_1 = \mu(\omega - n\Omega_0)/\omega$ and,

$$\mathbb{F}_R(k_x,t,\mathbf{u}) = -\frac{q}{m_0}\frac{L}{\Omega_0}\frac{\partial f_0}{\partial u_z}\,J_1\!\left(\frac{k_x u_\perp}{\Omega_0}\right)\exp\left(i\,\frac{(k_x+h_1)\,u_\perp}{\Omega_0}\sin\theta - i\theta\right)\exp\left(it\,\frac{u^2}{u_t^2}\right).$$

If we substitute this into (5.7) and use the Fourier expression, given in (3.9), for E_{1z}, then we may write g as,

$$g = \mathrm{Re}\int dk_x \int dk_x' \int_0^\infty dt \exp\left(i(k_x-k_x')x + i\xi_1 t\right) \mathcal{G}(k_x,k_x',t,\mathbf{u})\, E_{1z}(k_x)\, E_{1z}^*(k_x'),$$

(5.9)

where,

$$\mathcal{G} = -\frac{1}{2}\frac{q}{m_0}\frac{\Omega_0}{2\pi}\int_0^{2\pi/\Omega_0} d\tau \frac{\partial \mathbb{F}_R(k_x,t,\mathbf{u})}{\partial u_z} \exp\left(i\frac{(k_x-dk_x'+h_1 t)\,u_\perp}{\Omega_0}(\sin(\Omega\tau/\gamma-\theta)+\sin\theta)\right)$$

$$= \frac{1}{2}\frac{q^2}{m_0^2}\frac{\mu}{\omega} J_1\left(\frac{k_x u_\perp}{\Omega_0}\right) J_1\left(\frac{k_x' u_\perp}{\Omega_0}\right)\frac{\partial}{\partial u_z}\left(\frac{\partial f_0}{\partial u_z}\exp\left(it\frac{u^2}{u_t^2}\right)\right)$$

$$\times \exp\left(\frac{(k_x-dk_x'+h_1 t)\,u_\perp}{\Omega_0}\sin\theta\right). \qquad (5.10)$$

The power absorbed by the plasma can now be calculated from g by,

$$P = \int d^3\mathbf{u}\ \frac{1}{2} m_0 u^2\, g$$

$$= \mathrm{Re}\int dk_x \int dk_x' \int_0^\infty dt \exp\left(i(k_x-k_x')x + i\xi_1 t\right) \mathbb{P}(k_x,k_x',t,\mathbf{u})\, E_{1z}(k_x)\, E_{1z}^*(k_x'),$$

(5.11)

where,

$$\mathbb{P} = \int d^3\mathbf{u}\ \tfrac{1}{2} m_0 u^2\, \mathcal{G}$$

$$= \frac{1}{4}\frac{q^2}{m_0^2}\frac{\mu}{\omega}\int d^3\mathbf{u}\, u^2\ J_1\left(\frac{k_x u_\perp}{\Omega_0}\right) J_1\left(\frac{k_x' u_\perp}{\Omega_0}\right) J_0\left(\frac{(k_x - dk_x' + h_1 t)u_\perp}{\Omega_0}\right) \frac{\partial}{\partial u_z}\left(\frac{\partial f_0}{\partial u_z}\exp\left(it\frac{u^2}{u_t^2}\right)\right)$$

(5.12)

Proceeding in the same way as chapter 3 we assume a Maxwellian distribution and make the variable change $\mathbf{u}' = (\mathbf{u}/u_t)\,(1\text{-}it)^{1/2}$ and perform the θ and u_z integrations to give,

$$\mathbb{P} = \frac{\omega_p^2 \varepsilon_0}{4}\frac{\mu}{\omega}\frac{4}{(1\text{-}it)^{5/2}}\int_0^\infty du_\perp\, u_\perp\, J_1\left(\frac{k_x \rho u_\perp}{(1\text{-}it)^{1/2}}\right) J_1\left(\frac{k_x' \rho u_\perp}{(1\text{-}it)^{1/2}}\right)$$

$$\times\ J_0\left(\frac{(k_x - dk_x' + h_1 t)\rho u_\perp}{\Omega_0}\right)\exp(-u_\perp^2)\,. \qquad (5.13)$$

We now expand the Bessel functions out (see Appendix) to lowest order in the parameter ε (according to the ordering of (2.20)) which enables us to perform the $u_\perp$ integration,

$$\mathbb{P} = \frac{\omega_p^2 \varepsilon_0}{4}\frac{\mu\rho^2}{\omega}\frac{k_x k_x'}{(1\text{-}it)^{7/2}}\int_0^\infty du_\perp\, u_\perp^3 \exp(-u_\perp^2)$$

$$= \frac{\omega_p^2 \varepsilon_0}{8}\frac{\mu\rho^2}{\omega}\frac{k_x k_x'}{(1\text{-}it)^{7/2}}\,. \qquad (5.14)$$

This is now inserted back into the expression for the power absorbed (5.11), and the integrals can now be performed, using techniques similar to those in section 4.1, to give,

$$P = \frac{\omega_p^2 \varepsilon_0}{8} \frac{\mu\rho^2}{\omega} \operatorname{Im} F_{7/2}(\xi_1) \left| \frac{dE_1}{dx} \right|^2 . \qquad (5.15)$$

This is the power absorbed irreversibly by the plasma and we may make the following observations based on the properties of RPDF's , given in equation A.17. As $\operatorname{Im} F_q \leq 0$ for all real arguments, the real part of P is positive definite and so power always flows from the wave to the plasma, as we would expect for a plasma in thermal equilibrium. Further, as $\operatorname{Im} F_q = 0$ for positive real argument, no power is absorbed in the region where the electrons Larmor frequency is below the resonant frequency.

5.2.2 The Energy Equation.

Returning to the energy equation (5.4) and inserting the expression for the perturbed current density (4.13), we see that the time averaged equation for energy flow in the plasma is given by,

$$\frac{1}{2} \operatorname{Re} \left(\mathbf{E_1^*} \bullet \mathbf{J_1} \right) = - \frac{\omega_p^2 \varepsilon_0}{8} \frac{\mu\rho^2}{\omega} \operatorname{Im} F_{7/2}(\xi_1) \left| \frac{dE_1}{dx} \right|^2$$

$$+ \frac{d}{dx} \left(\operatorname{Im} \frac{\omega_p^2 \varepsilon_0}{8} \frac{\mu\rho^2}{\omega} F_{7/2}(\xi_1) E_{1z}^* \frac{dE_{1z}}{dx} \right) . \qquad (5.16)$$

We see that the expression for the energy flow is made up of two components. The first term we have already identified, in (5.12), as the power absorbed by the plasma. The remaining second term, is then, the kinetic power flux ($\nabla \bullet \mathbf{S}$) term. We see that it is indeed a derivative and integrates across the plasma to zero.

5.3 Self Consistency.

Having derived an energy conservation equation for our wave equation, we have shown that our equations are self consistent in the sense that they conserve energy. This should be contrasted with the wave equation produced by the inverse Fourier transform method (2.19),

$$\left(1 + \frac{1}{2}\frac{\omega_p^2}{\Omega^2} F_{7/2}\left(\frac{\mu x}{L}\right)\right)\frac{d^2E_{1z}}{dx^2} + \frac{\omega^2 - \omega_p^2}{c^2} E_{1z} = 0 . \tag{5.17}$$

The energy equation for this would be,

$$\frac{1}{2}\mathrm{Re}\left(\mathbf{E_1^*} \bullet \mathbf{J_1}\right) = -\frac{\omega_p^2 \varepsilon_0}{8}\frac{\mu\rho^2}{\omega}\,\mathrm{Im}\,F_{7/2}(\xi_1)\left|\frac{dE_1}{dx}\right|^2$$

$$+\,\mathrm{Im}\,F_{7/2}(\xi_1)\frac{d}{dx}\left(\frac{\omega_p^2 \varepsilon_0}{8}\frac{\mu\rho^2}{\omega} E_{1z}^* \frac{dE_{1z}}{dx}\right). \tag{5.18}$$

The first term can once again be identified as the power absorbed - by an analysis similar to section 5.2.1 - which should mean that the second term is due to the kinetic flux. However, it is clearly not a derivative and does not integrate across the plasma to zero, which indicates that the wave equation does not conserve energy. In this way we can say that the analysis, ignoring gyrokinetic effects, is not self consistent.

Although we shall not do so here, by forming an energy equation for the general wave equation (3.23) and calculating the corresponding power absorbed (in a manner similiar to section 5.2.1), it can be shown that all equations produced by our method are energy conserving, whereas those produced by a simple inverse Fourier transform are

generally not. The reason for this is that the inverse Fourier transform method ignores derivatives that should be acting on the equilibrium resonance functions (i.e. the RPDF's). Including the gyrokinetic correction in our analysis means that these derivatives are included in our final wave equations or, more precisely, tells us where to place the derivatives with respect to the perturbed electric field and the equilibrium resonance functions. If we look once more at (5.17) and (4.14), the equations produced by the two methods, we see that our method has shown us that one of the derivatives in (5.17) should be placed to the left of the bracketed term and so act also on the RPDF.

6. NUMERICAL ANALYSIS.

Having obtained wave equations, in chapter four, which describe the propagation of plasma waves through resonances of interest for tokamak heating, we now wish to solve them numerically. This requires the integrating of the equations across their resonance which can, especially for the fourth and sixth order equations, require large amounts of computing time. The numerical integration was performed using a finite-difference method available through the NAG library. Before looking at our results we shall consider the question of boundary conditions.

6.1 Boundary conditions.

We wish then to use the equations of chapter four to analyse, numerically, the propagation of waves through electron cyclotron resonances. To do so we must consider the boundary conditions for the various equations. Essentially, we wish to consider the effects of a single mode being launched into the system and measure the extent to which it is reflected or mode converted. In all cases our method is basically the same and starts from our assumption that away from resonance our WKB model, of section 2.2.1, applies.

Starting with the O-mode, we have a second order differential equation (4.14) which requires two complex boundary conditions. If we take the asymptotic limit to the WKB approximation (equation (4.15)) of the full wave equation, we have,

$$\frac{1}{x}\left(\frac{1}{2}\frac{L}{\mu}\frac{\omega_p^2}{\Omega_0^2}k_x^2\right) + k_x^2 - \frac{\omega^2 - \omega_p^2}{c^2} = 0\,, \qquad (6.1)$$

which is plotted in figure (6.1). We see that far from resonance, as $x \to \pm\infty$, we have four wave branches, two inwardly propagating and two outwardly propagating. Of the inwardly propagating branches; the left hand one corresponds to a high field incident (HFI) wave and the right hand one to a low field incident (LFI) wave. Our boundary conditions are then, to set one of these branches to zero and one to unit amplitude, dependent upon which direction of propagation we wish to analyse. Information on the transmission and reflection can then be calculated from the amplitude of the outgoing waves.

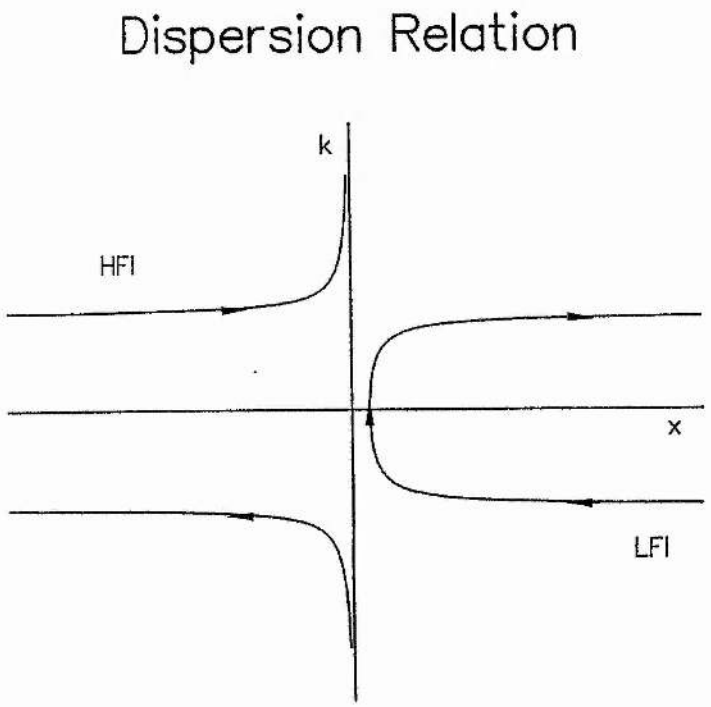

Figure 6.1

Dispersion relation for the O-mode at perpendicular propagation

For the X-mode the situation is complicated by the existence of the Bernstein wave. Our full wave equation is now of fourth order and so requires four complex

boundary conditions. If we take the asymptotic limit of the WKB solution to such equations (either equations (4.25,26) or equations (4.31,32)) our dispersion relation takes the form,

$$\frac{1}{x}\left(Ak_x^4 + Bk_x^2 + C\right) + (k_x^2 - k_0^2) = 0\,. \qquad (6.2)$$

where k_0 is the wave number for the cold X-mode. A model dispersion relation for such an equation is plotted in figure (6.2). We see that, far from resonance, we now have six wave branches, three inwardly and three outwardly propagating. The four closest to the axis correspond to the X-mode and the other two correspond to the Bernstein mode.

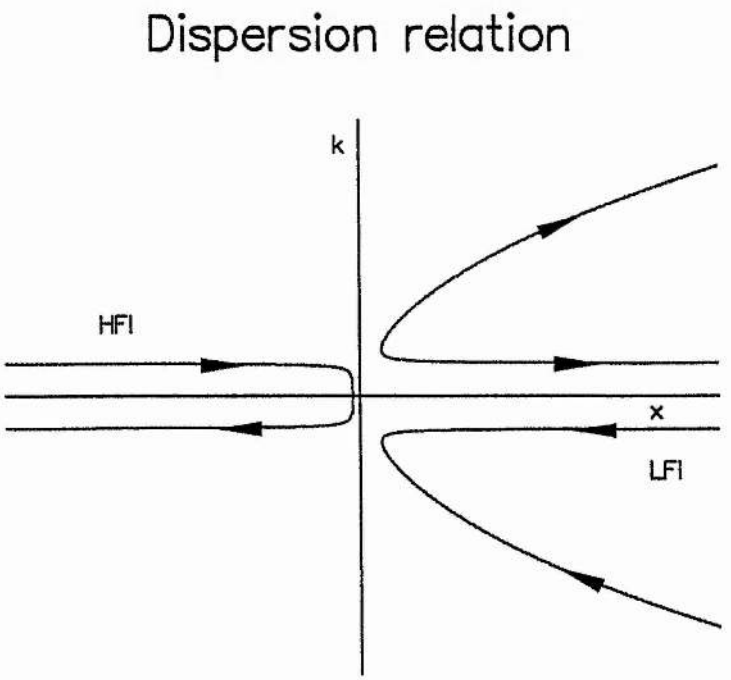

Figure 6.2

Dispersion relation for the X-mode at perpendicular propagation

The Bernstein mode tends, in the limit $x \to \pm\infty$, to the form $k^2 \propto x$. For $x>0$ this gives us two wave branches, but for $x<0$ the mode is evanescent and we have an exponentially growing and exponentially decaying solution. So, our boundary conditions are to set one of the X-mode incoming waves to zero and one to unity (dependent on which we wish to analyse), the incoming Bernstein wave to zero and the exponentially growing (physically unreal) mode to zero. This gives us the required four boundary conditions, two on either side of the resonance.

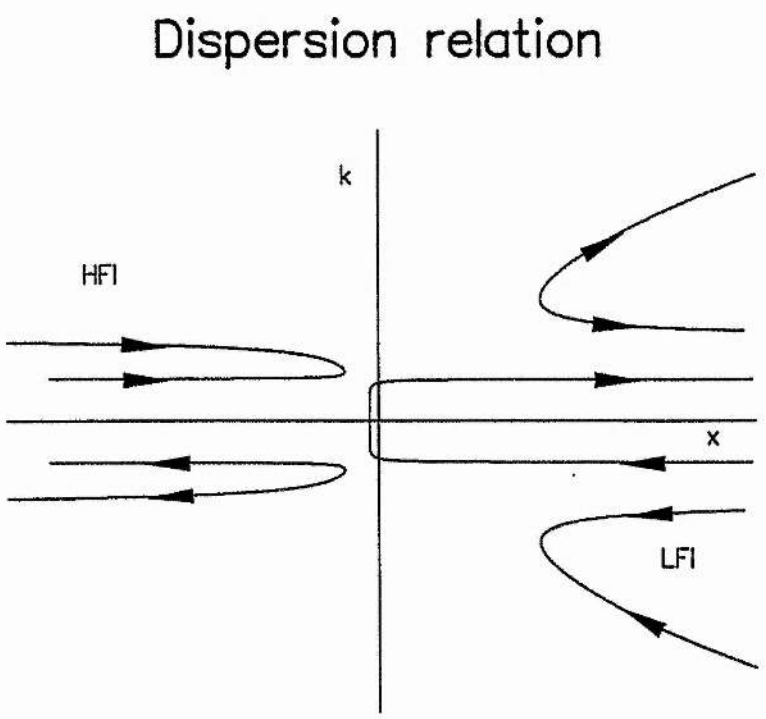

Figure 6.3

Dispersion relation for oblique propagation

Finally, for oblique propagation through the fundamental, we have an asymptotic dispersion relation of the form,

$$\frac{1}{x}\left(Ak_x^6 + Bk_x^4 + Ck_x^2 + D\right) + (k_x^2 - k_{ord}^2)(k_x^2 - k_{ex}^2) = 0. \qquad (6.3)$$

where k_{ord} is the wave number for the cold O-mode and k_{ex} is the wave number for the cold X-mode. Looking at the model dispersion relation, in figure (6.3), we see we now have ten wave branches. The eight nearest the axis represent the O-mode and X-mode, with the two outer branches representing the Bernstein mode. Once again the Bernstein mode is evanescent as $x \rightarrow -\infty$, and has a physically unreal solution. Thus, our boundary conditions are to set one of the four incoming waves in the ordinary or extra-ordinary modes to one, the other three to zero, the incoming Bernstein wave to zero and the exponentially growing solution to zero. This gives us the required six boundary conditions.

6.1 ECRH at the fundamental resonances

As discussed earlier, a large amount of experimental work has and is being carried out into the use of electron cyclotron heating as an auxiliary heating scheme for tokamaks. One experimental reactor which currently uses such a scheme is COMPASS. We shall take its parameters (given in table 6.1) for the purpose of this study.

Table 6.1

Typical parameters for COMPASS

Magnetic field	2.4 T
Electron density	10^{19} - 5×10^{19} m^{-3}
Electron temperature	600 eV - 3 keV
Major radius	0.557 m
Minor radius	0.10 m

6.1.1 O-mode heating at the fundamental resonance.

We consider first heating through an ordinary wave launched perpendicularly to the magnetic field at the fundamental resonance. Previous experiments (for instance the work by Efthimion et al (1980) on the Princeton Large Torus) have shown that energy can be absorbed very effectively by such a method. WKB theory predicts that the opacity is given by,

$$\tau = 2 \int_{-\infty}^{\infty} dx\, \delta k_I = \frac{\pi}{2} \frac{\omega_p^2}{\Omega_0^2} \frac{k_0 L}{\mu} , \qquad (6.4)$$

and so for significant absorption we require that the absorption width L/μ is of the order of the wavelength.

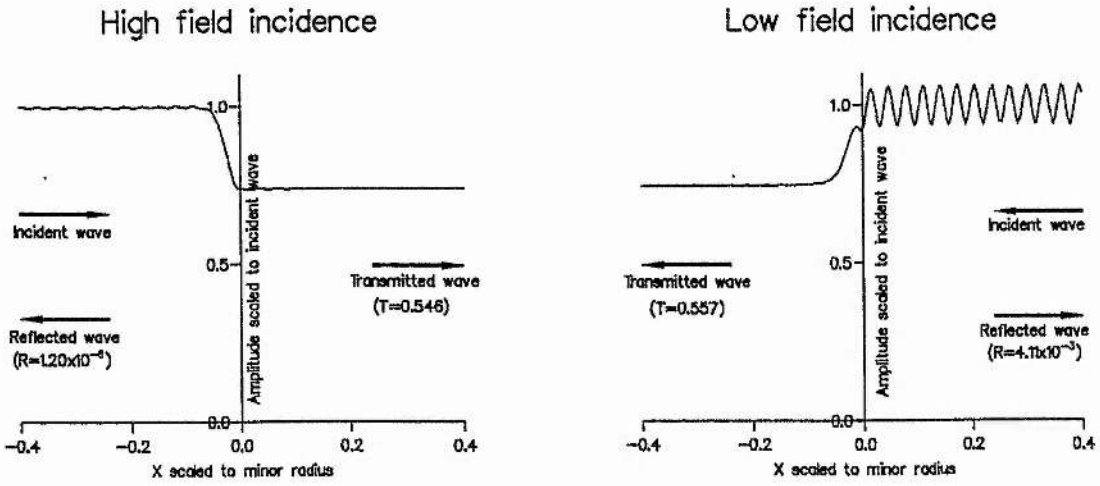

Figures 6.4a and 6.4b

Wave profiles for O-mode at the

fundamental, $n_0 = 10^{19}$ m^{-3}, T = 600eV,

B = 2.4 T and L = 0.557 m.

In figures 6.4a and 6.4b we see two wave profiles for ordinary waves passing through the fundamental, as calculated by integrating equation (4.14). Qualitatively, we see that our results are in agreement with WKB theory. For high field incidence we have negligible reflection ($R=1.20\times10^{-6}$) and so the energy is either transmitted or absorbed. For low field incidence, however, we do see (through its interference with the incident wave) significant reflection ($R=4.11\times10^{-3}$). However, we note that this reflection is less than would be predicted by WKB theory (R=0.196) and also that, although the transmission coefficients for the high and low field incidence are in close agreement (to about 2%), the high field transmission is slightly larger (generally the case).

Looking in more detail at the power absorption, given in figures 6.5a and 6.5b, we see the local emission discussed in chapter four. As predicted, for high field incidence we see a region ahead of the resonance in which energy is flowing from the plasma to the wave.

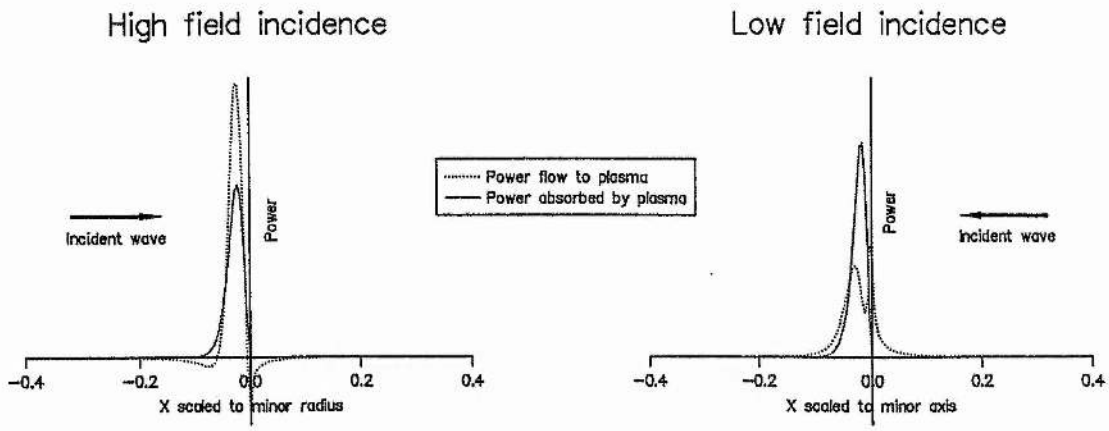

Figures 6.5a and 6.5b

Power profiles for O-mode at the

fundamental, $n_0 = 10^{19}$ m^{-3}, T = 600eV,

B = 2.4 T and L = 0.557 m.

However, we reiterate that this is not due to any source of free energy within the plasma, but rather the return of the excess of energy absorbed at the absorption peak. For low field incidence we see the reverse case, in which an excess of energy is absorbed ahead of the resonance and returned at the absorption peak. We also note that the absorption profiles themselves differ for varying incidence, a fact that is shown more clearly in figure 6.6 where the profiles have been plotted on the same axes.

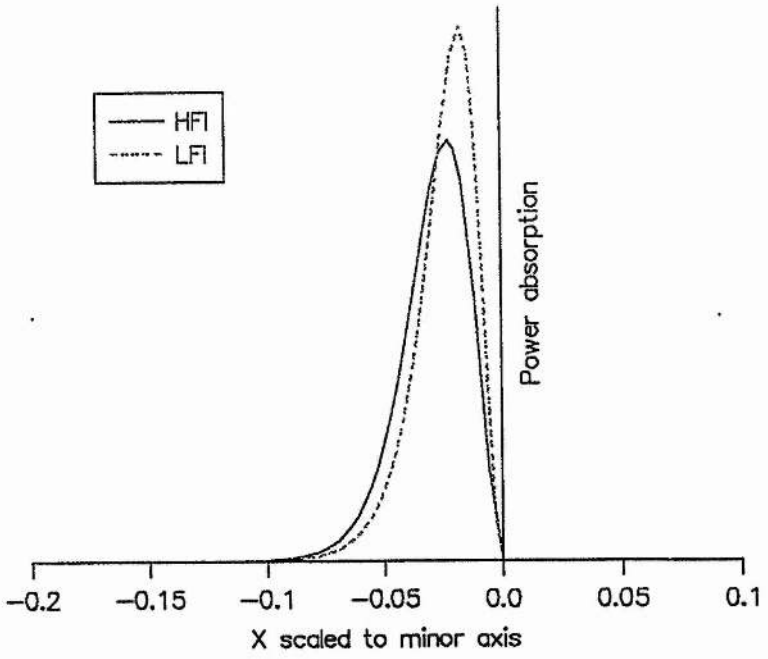

Figure 6.6

Absorption profiles for O-mode at the fundamental, $n_0 = 10^{19}$ m^{-3}, T = 600eV, B = 2.4 T and L = 0.557 m.

In general, however, we have good agreement between the full wave equations and the WKB model. Figure 6.7 shows the absorption occurring at various temperatures

with typical COMPASS parameters, the boxes indicating the full wave results and the curve the WKB theory.

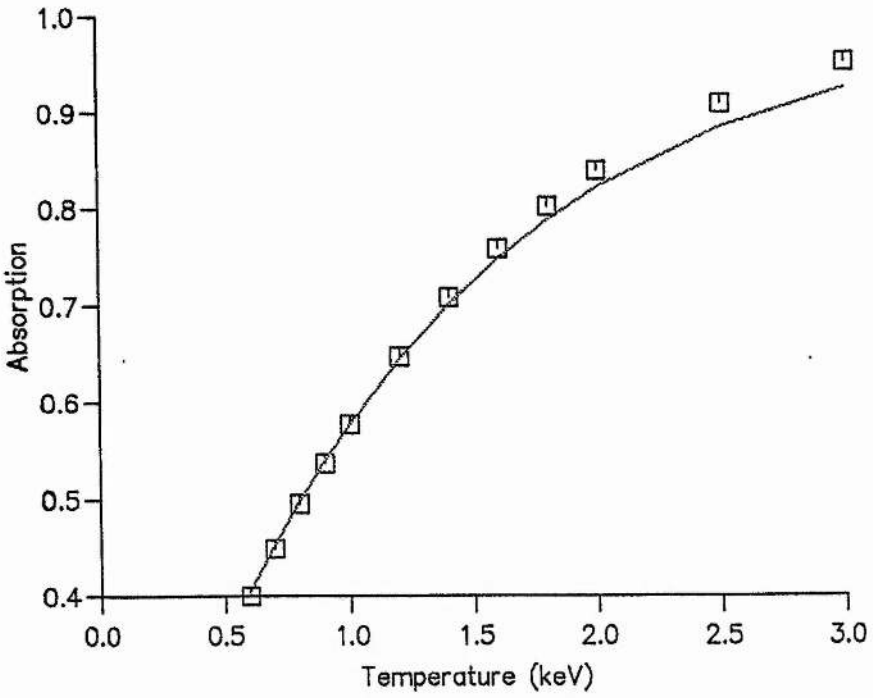

Figure 6.7

Absorption for O-mode at the fundamental,

$n_0 = 10^{19}$ m^{-3}, B = 2.4 T,

L = 0.557 m and low field incidence.

Despite higher than predicted absorption at higher temperatures, the fit is close. This is principally due to the low level of reflection for all parameters.

For propagation oblique to the gradient (equation (4.20)), we see similar results. Reflection is slight and transmission is in good agreement with WKB theory. As we

increase the wave number perpendicular to the gradient (k_y) absorption decreases and transmission increases until cut-off is reached (figure (6.8)).

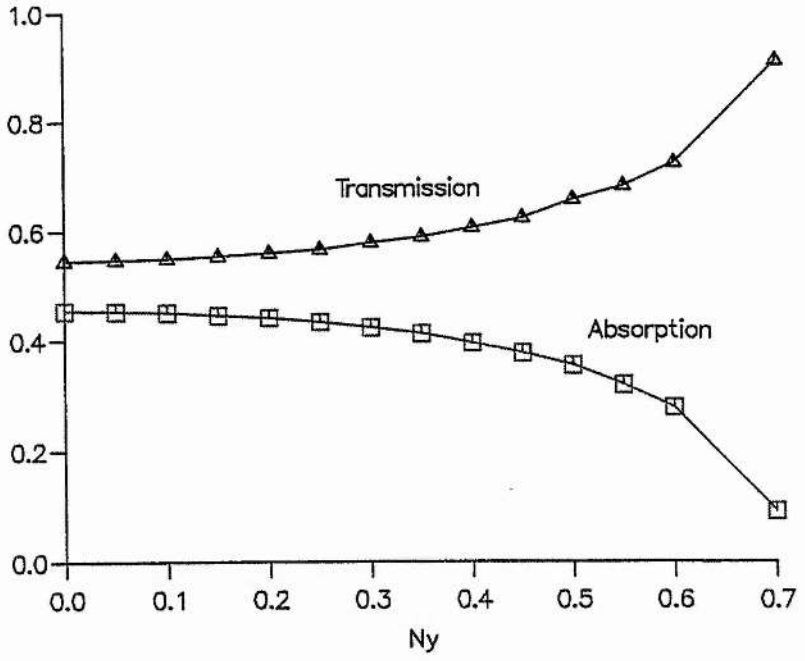

Figure 6.8

Profiles for O-mode at the fundamental

$n_0 = 1.2\times10^{19}$ m^{-3}, B = 2.4 T, T=600 eV,

L = 0.557 m and low field incidence.

6.1.2 X-mode heating at the first harmonic resonance.

We look now at heating at the first harmonic resonance. Here, the wave dynamics are dominated by the interaction between the first harmonic and the nearby upper-hybrid resonance. In cold plasma theory, the first harmonic ($\omega=\Omega$) cancels from the equations and we are left instead with the upper-hybrid resonance ($\omega=\sqrt{(\omega_p^2+\Omega^2)}$). For $\omega_p<\Omega$, the case of interest in heating schemes, the two resonances lie close together. One result of

the cancelling of the cold plasma effect of the first harmonic is that, in WKB theory, the resonance is an order lower than those of fundamental O-mode or second harmonic X-mode heating, being given by,

$$\tau = \frac{\pi}{4}\frac{\omega_p^2}{\Omega_0^2}\frac{\omega}{c}\frac{L}{\mu^2}\left(2-\frac{\omega_p^2}{\Omega_0^2}\right)^{1/2}, \qquad (6.5)$$

which is, in general, small ($\tau \sim 10^{-3}$ for typical COMPASS parameters).

Table 6.2

Wave coefficients for X-mode at the fundamental.

B = 2.4 T, T=600 eV and L = 0.557 m.

Density (m^{-3})	**Incidence**	**R**	**T**	**A**
2.0×10^{16}	HFI	6.91×10^{-4}	0.352	0.348
2.0×10^{16}	LFI	9.83×10^{-5}	0.360	0.640
1.0×10^{19}	HFI	0.17	7.13×10^{-2}	0.757
1.0×10^{19}	LFI	1.00	1.84×10^{-13}	8.09×10^{-7}

Looking at the results from the full wave equation in the low and high density regimes (Table 6.2) we see that for low density ($n_0 = 2.0\times10^{16}$, plasma frequency is well below the cyclotron frequency) we have good agreement with WKB theory. Waves, from either direction, can tunnel through the evanescent region between the upper-hybrid and the cut-off and very little energy is absorbed.

For higher densities ($n_0 = 1.0\times10^{19}$, typical of those in COMPASS) the situation is more complicated. For the low field case we still have, as we would expect from WKB

theory, virtually total reflection, which takes place at the cutoff. For high field incidence, though, the case is different. Transmission is still low, but reflection is now significantly reduced, with a large amount of the wave energy absorbed. This, as noted by Petrillo et al (1987), is due to the extraordinary wave being converted to a Bernstein wave at the upper-hybrid resonance, and travelling back to the first harmonic resonance where it is absorbed. This is illustrated in figure (6.9) where we have plotted the spatial dependence of the x-component of the perturbed electric field, in which the Bernstein mode is carried.

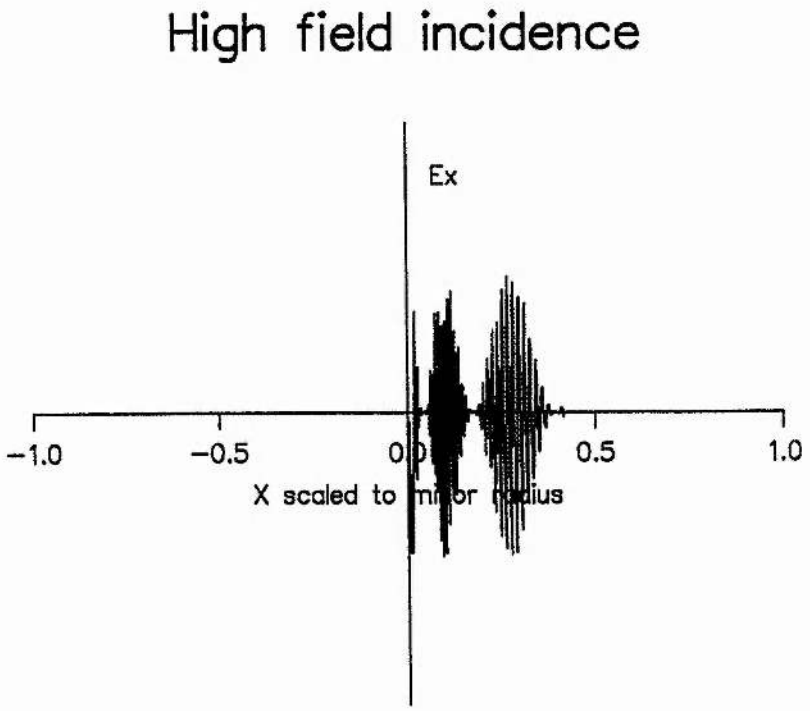

Figure 6.9

Wave profile for X-mode at the first harmonic, B = 2.4 T, T=600 eV, $n_0 = 1.0\times10^{19}$ and L = 0.557 m.

For oblique propagation we must solve the sixth order wave equation, a process that takes considerable computing time primarily because of the small scale of the Bernstein wavelengths. The numerical results show good agreement with the previous full wave calculation of Lampis et al (1987), with little conversion from the X-mode to the O-mode and correlation with the WKB theory for low field incidence. For high field incidence, a similar high absorption to that for perpendicular propagation is seen at small angles, which diminishes as the Doppler width approaches the relativistic absorption width. In figure (6.10) we illustrate the wave profile for an X-mode with high field launch at $\theta = 5°$. We see a similar profile to that of (6.9) with a Bernstein wave propagating back to the first harmonic resonance where it is absorbed.

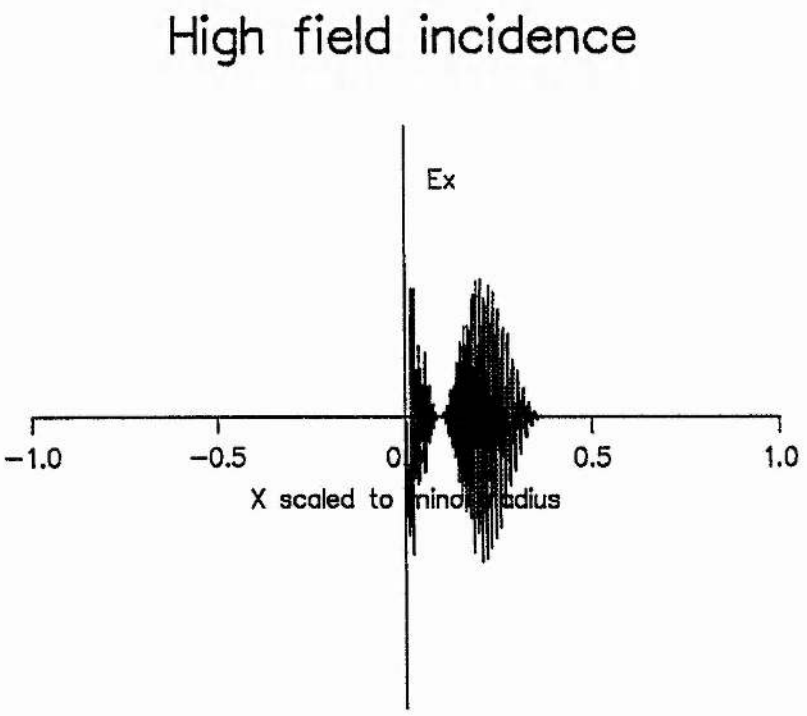

Figure 6.10

Wave profile for X-mode at first harmonic,

B = 2.4 T, T=600 eV, $n_0 = 1.0\times10^{19}$,

L = 0.557 m and $\theta = 5°$.

6.1.3 Discussion.

Absorption at the O-mode has been shown to be in line with that predicted by WKB theory, both for propagation parallel and oblique to the magnetic field gradient. For low field incidence the reflection measured has been shown to be somewhat less than WKB would predict.

For the X-mode, we have shown that - consistent with WKB theory - effective heating cannot occur for low field incidence. Undoubtedly the most interesting result, though, is the large amount of energy which can be absorbed at the fundamental X-mode, for high field incidence, when compared with WKB theory. This is known to be a result of mode conversion at the fundamental, an effect which cannot be described by WKB theory.

6.2 The ECA Diagnostic In The JET Divertor.

In (1993) a pumped divertor was added to the JET experiment. To monitor its effectiveness, a number of diagnostics were required, one of which, the Electron Cyclotron Absorption (ECA) diagnostic (Smith et al (1992)), involved measuring the electron temperature through the absorption of an electron cyclotron wave. The electron pressure was calculated from the diagnostic by means of a WKB model and here we wish to look at the validity of this using our full wave theory.

A divertor is a device for reducing the impurity levels in a tokamak. By impurities, we mean any heavy ions that may be present in the plasma. These usually come from the chamber wall and their presence, in even minute concentrations, can have

serious effects upon the stability of the plasma. A divertor consists of a side chamber to the reactor into which the magnetic field lines are deformed. Thus, escaping plasma enters the divertor and the impurities are removed by a pumping system. Such a system is currently being added to JET and to measure its effectiveness a number of diagnostics are required. A set of typical values for parameters in this divertor is given below.

Table 6.3

Typical parameters for the JET Pumped Divertor.

Magnetic field	3 T
Electron density	10^{19} - 2 x 10^{20} m^{-3}
Electron temperature	10 - 100eV
Magnetic field length scale	3 m

Temperature measurements in plasmas are usually done by diagnostics based on the principle of electron cyclotron emission (ECE). Such diagnostics are passive and are basically radiation receivers that measure the amount of power emitted by the plasma in a given frequency range. The temperature of the plasma can then be calculated from the amount of power emitted. However, such diagnostics are only effective if the plasma is optically thick (that is to say, $\tau >> 1$, where τ is the optical depth). To see why this is so we need only to consider the case of an optically thin ($\tau << 1$) plasma. In such a case, energy emitted deeper in the plasma would still reach the sensor without absorption and so will contaminate any measurement. In the JET pumped divertor this is certainly the case. The plasma is optically thin ($\tau \sim 0.1$, for the second harmonic X-mode) and most of the radiation reaching the probe is from the hotter main plasma. As a result, an ECA diagnostic was selected.

To use an ECA diagnostic to measure the temperature of a plasma, a theory must be developed for relating the wave transmission to the temperature. The simplest way to do this would be through a WKB analysis. If such an analysis were not valid, the absorption would be likely to depend in a more complicated way on parameters such as the density and magnetic profile. Such a situation would reduce the effectiveness of the diagnostic. Here, we use the full wave equation for the second harmonic to test the validity of a WKB analysis for the regime of interest.

We wish then to compare the transmission coefficient calculated from WKB theory with that of the full wave equation (4.31,32). For a plasma in the presence of a linear magnetic field gradient the opacity (τ) for the second harmonic resonance, calculated from a WKB approximation, is,

$$\tau = 2\pi\,\alpha^2 \frac{\omega}{c} \frac{L}{\mu} \frac{(3-2\alpha^2)^2}{(3-4\alpha^2)^2} \left(\frac{4(1-\alpha^2)^2 - 1}{3-4\alpha^2} \right)^{1/2}, \qquad (6.6)$$

as given by Bornatici et al (1983). The transmission coefficient is then calculated from this by $T=\exp(-\tau)$.

6.2.1 Results.

Integration of the full wave equations for the X-mode at the second harmonic resonance, show little conversion to Bernstein modes with most of the wave energy remaining in the X-mode or being absorbed. Consequently, we find good agreement with the WKB theory, particularly with regards to the transmission coefficient. Figure (6.11) shows the E_x profile for the propagation of a typical wave through the resonance. We see evidence of conversion to Bernstein waves in a small layer around the second harmonic

resonance, but not on the scale of that for the fundamental. This is typical for all such profiles.

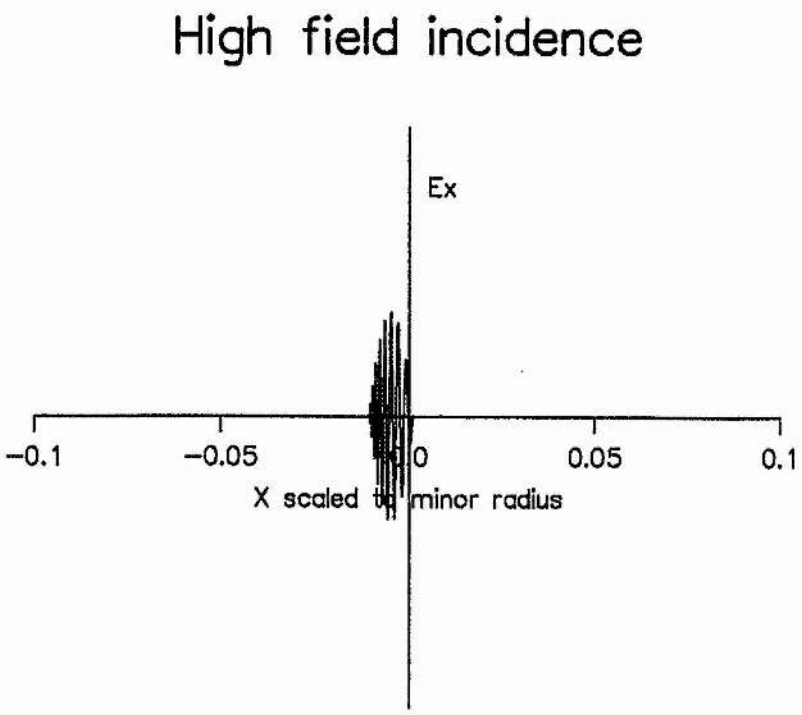

Figure 6.11

Wave profile for X-mode at second harmonic, B = 3.0 T, T=100 eV, $n_0 = 1.0\times10^{19}$, L = 3.0 m.

Consistency between the WKB and full wave theories was tested over the range of parameters for which the diagnostic was to be used and close agreement was found throughout. Differences were generally of the order of a few percent, with the largest discrepancy being around 7%. In figure (6.12) we illustrate the closeness of the fit between WKB theory over a range of densities. We see that the fit is almost exact for high transmission and even for low transmission the theories differ by only a few percent.

In general we also see that the low field incidence fit is closer than that for high field incidence.

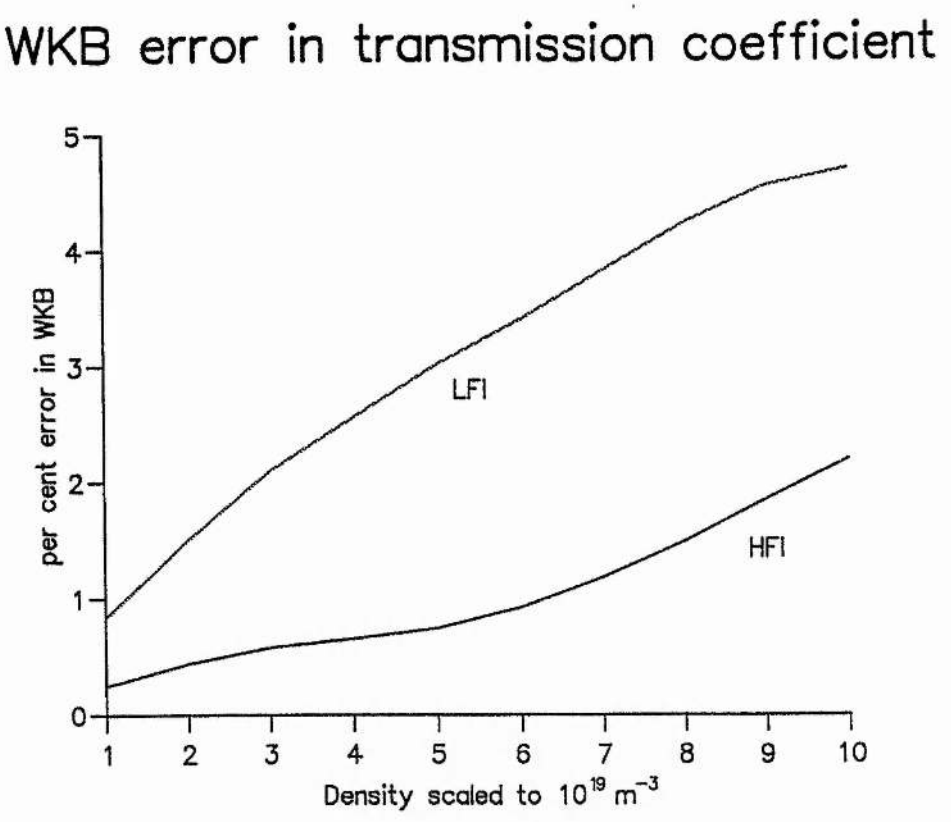

Figure 6.12

Consistency between WKB and full wave results for transmission coefficient.

B = 2.4 T, T=100 eV, L = 3 m.

6.2.2 Discussion.

Despite the existence of discrepancies between the WKB theory and the full wave calculation, it would appear that WKB is accurate to within the 10% required for the diagnostic. Mode conversion to Bernstein waves is clearly taking place but, as opposed to

the fundamental resonance, this is not affecting the transmission. Indeed, the transmission coefficient would appear to be the most rugged of plasma wave parameters.

7. EXTENSION TO OTHER GEOMETRIES.

The slab model with linear magnetic gradient, used so far, is a much simplified version of the actual geometry of a Tokamak plasma. However, this approximation has illustrated perfectly adequately the necessity of including the gyrokinetic correction for a self consistent treatment of wave propagation in an inhomogeneous plasma. We now consider how to extend such an analysis to more complicated geometries by use of the gyrokinetic theory.

At this stage the difference between the gyrokinetic correction and the gyrokinetic theory should be emphasised to avoid future confusion. The gyrokinetic correction, as explained in chapter 2, was introduced by Lashmore-Davies and Dendy (1989) with an analysis based on the gyrokinetic theory, but the correction can be used in an analysis without the gyrokinetic theory, such as in chapter two of this work.

The gyrokinetic theory, however, is a formalism developed, independently by Rutherford and Frieman (1968) and Taylor and Hastie (1968), to describe the propagation of electromagnetic waves in general plasma geometries. It is essentially a transformation of the equations of kinetic theory from the particle phase space to the more natural guiding-centre phase space. A good account can be found in Chen and Tsai (1983) or Chen (1987).

The original treatment was non-relativistic, but Tsai et al (1984) extended the formalism into the high frequency, hence relativistic, regime. In this chapter it is shown how to include the gyrokinetic correction in the gyrokinetic formalism at high frequencies, where its appearance is considerably more natural, and so gives a method for extending the analysis to more complicated geometries.

7.1 The Gyrokinetic Formalism.

In this section we review the work of Tsai et al (1984) and the reader is referred to this paper. We begin by defining the guiding-centre phase space (**X**,**U**) in terms of the particle phase space (**x**,**u**) by the transformation,

$$\mathbf{X} = \mathbf{x} + \mathbf{u} \times \mathbf{e}_{\parallel} / \Omega, \tag{7.1}$$

$$\mathbf{U} = (\varepsilon, \mu, \alpha), \tag{7.2}$$

where $\mu = u_{\perp}^2/2B$, $\varepsilon = c^2\gamma + q\Phi_0/m_0$; $\mathbf{u} = \gamma\mathbf{v}$ and $\mathbf{U} = \gamma\mathbf{V}$ are the relativistic velocities; m_0 is the rest mass; $\Omega = qB/m_0$, $\mathbf{e}_{\parallel} = \mathbf{B}/B$; α is the gyrophase angle, and,

$$\gamma = (1 + v^2/c^2)^{-1/2} = \frac{1}{c^2}(\varepsilon - q\Phi_0/m_0), \tag{7.3}$$

$$u_{\parallel}^2 = -2B\mu + (\varepsilon - q\Phi_0/m_0)^2/c^2 - c^2, \tag{7.4}$$

$$\mathbf{u}_{\perp} = u_{\perp}(\mathbf{e}_1 \cos\alpha + \mathbf{e}_2 \sin\alpha), \tag{7.5}$$

with $\mathbf{e}_1$, $\mathbf{e}_2$ and $\mathbf{e}_{\parallel}$ being the local orthogonal unit vectors. Φ_0 and **B** are the equilibrium electrostatic and magnetic field, respectively.

The unperturbed Vlasov Propagator in particle phase space is,

$$L_u = \gamma\frac{\partial}{\partial t} + \mathbf{u}\cdot\nabla_x + (\mathbf{u}\times\Omega)\cdot\nabla_u + \frac{q}{m_0}\gamma\mathbf{E}_0\cdot\nabla_u, \tag{7.6}$$

and in guiding-centre phase space becomes,

$$L_g = \gamma\frac{\partial}{\partial t} + u_{\|}\,\mathbf{e}_{\|}\bullet\nabla_{\mathbf{X}} + \mathbf{u}\bullet(\lambda_{B_1}+\lambda_{B_2}) - \Omega\frac{\partial}{\partial\alpha} + \frac{q}{m_0}\gamma\,\mathbf{E_0}\bullet\left[\frac{\mathbf{u}_\perp}{B}\frac{\partial}{\partial\mu} + \frac{\mathbf{e}_\alpha}{u_\perp}\frac{\partial}{\partial\alpha}\right]$$

$$+\gamma\,\mathbf{v_E}\bullet\nabla_{\mathbf{x}}\,, \tag{7.7}$$

where,

$$\lambda_{B_1} = \mathbf{u}\times\nabla_{\mathbf{x}}(\mathbf{e}_{\|}/\Omega)\bullet\nabla_{\mathbf{X}}\,, \tag{7.8}$$

$$\lambda_{B_2} = -\left[\frac{\mu}{B}\nabla_{\mathbf{x}}B + \frac{u_{\|}}{B}\nabla_{\mathbf{x}}\,\mathbf{e}_{\|}\bullet\mathbf{u}_\perp\right]\frac{\partial}{\partial\mu}$$

$$+\left[(\nabla_{\mathbf{x}}\,\mathbf{e_2})\bullet\mathbf{e_1} + \frac{u_{\|}}{u_\perp^2}\nabla_{\mathbf{x}}\,\mathbf{e}_{\|}\,(\mathbf{u}_\perp\times\mathbf{e}_{\|})\right]\frac{\partial}{\partial\alpha}\,, \tag{7.9}$$

$$\mathbf{E_0} = -\nabla_{\mathbf{x}}\,\Phi_0, \qquad \mathbf{v_E} = \frac{\mathbf{E_0}\times\mathbf{e}_{\|}}{B}, \qquad \mathbf{e}_\alpha = -\mathbf{e_1}\sin\alpha + \mathbf{e_2}\cos\alpha. \tag{7.10}$$

$\mathbf{v_E}$ is clearly the E-field relativistic drift velocity. The equations are now expanded in terms of the small parameter $\rho/L \ll 1$ and solved to first order. The distribution function (F_g) is then,

$$F_g = F_{g0} + F_{g1} + O(\rho^2/L^2)\,, \tag{7.11}$$

where the equilibrium distribution function (F_{g0}) is given by,

$$F_{g0} = F_{g0}(\varepsilon,\mu,\mathbf{X})\,. \tag{7.12}$$

r distribution function (the α dependent part, $\tilde{F}_{g1}$)

(7.13)

$$\frac{\cdot\nabla_x e_\parallel \bullet u_\perp) - \frac{1}{2}u_\perp^2 \nabla_x \bullet e_\parallel}{\Omega}, \tag{7.14}$$

(7.15)

$$\frac{e_\parallel \bullet \nabla_x e_\parallel}{\quad}, \tag{7.16}$$

tivistic drift velocity due to gradient and curvature
stic drift velocity, incorporating the E-field drift as
hus becomes,

$$\left(\delta a_g \times \nabla e_\parallel / \Omega\right) \bullet \nabla_X \Big) F_g, \tag{7.17}$$

(7.18)

onse from the equation by the transformation,

(7.19)

where,

$$\delta F_{ag} = \frac{q}{m_0}\left(\delta\Phi_g \frac{\partial}{\partial\varepsilon} + \left(\gamma\,\delta\Phi - u_\parallel\,\delta A_\parallel\right)_g \frac{1}{B}\frac{\partial}{\partial\mu} + \frac{\delta\mathbf{A_g}\times\mathbf{e_\parallel}}{\Omega}\bullet\nabla_{\mathbf{X}}\right)F_{g0}\ , \qquad (7.20)$$

and $\delta\Phi_g$ and $\delta\mathbf{A_g}$ are the perturbed field potential and vector potential respectively. Equation (7.17) is, thus, of the from,

$$L_g\,\delta G_g = -R_g\,, \qquad (7.21)$$

where the expression for R_g is given in Tsai et al (1984) equations (23-29). The complexity of R_g makes solution extremely difficult, but we can simplify by introducing the ordering,

$$\gamma\left|\frac{\partial}{\partial t}\right| \sim u_t\left|\mathbf{e_\parallel}\bullet\nabla_{\mathbf{X}}\right| \sim u_t\left|\mathbf{e_\parallel}\times\nabla_{\mathbf{X}}\right| \sim |\Omega| \sim O(1)\,, \qquad (7.22)$$

and by expressing the resonant terms, δG_g , in the perturbed current density, in terms of their Fourier components with respect to the gyrophase angle, α ; That is,

$$\delta G_g = \sum_{\ell=-\infty}^{\infty} \langle\delta G_g\rangle_\ell \exp(-i\ell\alpha)\,. \qquad (7.23)$$

With the further transformation,

$$\langle\delta G_g\rangle_\ell = -\frac{q}{m_0 B}\frac{\partial F_{g0}}{\partial\mu}\langle\delta\psi_g\rangle_\ell + \langle\delta H_g\rangle_\ell\ , \qquad (7.24)$$

where,

$$\delta\psi_g = \gamma\,\delta\Phi_g - \mathbf{u}\bullet\delta\mathbf{A_g}\ , \qquad (7.25)$$

the final form of the linearised Vlasov equation becomes,

$$\langle L_g\rangle_\ell \langle \delta H_g\rangle_\ell = -\frac{q}{m_0}\left(\langle S_1\rangle_\ell + \langle S_2\rangle_\ell \delta_{\ell,0}\right), \tag{7.26}$$

where,

$$\langle L_g\rangle_\ell = (\hat{u}_\parallel \mathbf{e}_\parallel + \mathbf{u_D})\bullet\nabla_x - i(\gamma\omega - \ell\Omega + \ell\omega_\alpha), \tag{7.27}$$

$$\langle S_1\rangle_\ell = -i\left(\omega\frac{\partial F_{g0}}{\partial\varepsilon} + \frac{\ell\Omega}{B}\frac{\partial F_{g0}}{\partial\mu} + i\nabla_X F_{g0}\bullet(\mathbf{e}_\parallel/\Omega)\times\nabla_X\right)\langle\delta\psi_g\rangle_\ell, \tag{7.28}$$

$$\begin{aligned}\langle S_2\rangle_\ell = \Big(& u_\parallel\langle \mathbf{e}_\parallel\bullet\nabla_X\delta\psi_g\rangle_\ell - u_\parallel\mathbf{e}_\parallel\bullet\nabla_X\langle\delta\psi_g\rangle_\ell - \mathbf{u_D}\bullet\nabla_X\langle\delta\psi_g\rangle_\ell \\ & - \left(\gamma\langle\mathbf{u}_\perp\delta\Phi_g\rangle_\ell + \langle\mathbf{u}\bullet\delta\mathbf{A_g}\rangle_\ell u_\parallel\mathbf{e}_\parallel - u_\parallel\langle\mathbf{u}\,\delta A_{\parallel g}\rangle_\ell\right)\bullet\nabla_X \ln B \\ & + \langle(\nabla_U\tilde{\beta})\bullet\left(\nabla_X(\mathbf{u}\bullet\delta\mathbf{A_g}) - (\mathbf{u}\bullet\nabla_X\delta\mathbf{A_g}) - \gamma\delta\Phi_g\right)\rangle_\ell \\ & - u_\parallel\langle(\mathbf{u}\bullet\nabla_X\mathbf{e}_\parallel)\bullet\delta\mathbf{A_g}\rangle_\ell + \langle\delta A_{\parallel g}(\mathbf{u}\bullet\nabla_X)\rangle\,\mathbf{e}_\parallel\bullet\mathbf{u})_\ell \\ & + \frac{q}{m_0}\left(\mathbf{E_0}\bullet\langle\mathbf{u}\,\delta\Phi_g\rangle_\ell - \gamma E_{0\parallel}\langle\delta A_{\parallel g}\rangle_\ell\right) + i\ell\omega_\alpha\langle\delta\psi_g\rangle_\ell \\ & + \Omega\left(\langle(\tilde{\beta}\,\delta\Phi_g)_{\alpha'}\rangle_\ell\left(\frac{\partial}{\partial\varepsilon} + \frac{\gamma}{B}\frac{\partial}{\partial\mu}\right)\right. \\ & \left. - \langle(\tilde{\beta}\,u_\parallel\,\delta A_{\parallel g})_{\alpha'}\rangle_\ell\frac{1}{B}\frac{\partial}{\partial\mu}\right)\Big)\frac{1}{B}\frac{\partial F_{g0}}{\partial\mu},\end{aligned} \tag{7.29}$$

$$\hat{u}_\parallel = u_\parallel + \frac{u_\perp^2}{2\Omega}\,\mathbf{e}_\parallel\bullet\nabla_x\times\mathbf{e}_\parallel, \tag{7.30}$$

$$\omega_\alpha = \langle\mathbf{u}\bullet\nabla_X\alpha\rangle_0 = u_\parallel\left(\mathbf{e_1}\bullet(\mathbf{e}_\parallel\bullet\nabla_x\mathbf{e_2}) - \frac{1}{2}\mathbf{e}_\parallel\bullet(\nabla_x\times\mathbf{e}_\parallel)\right). \tag{7.31}$$

$\hat{u}_\parallel$ is the effective guiding centre velocity and ω_α is the correction to the cyclotron frequency due to bending of any co-ordinate system about a field line.

The general problem is, then, to solve equation (7.26) self-consistently with Maxwell's field equations. This is by no means easy but, for complicated geometries, the equations provide the most convenient form of solution. In the next section we shall show how the gyrokinetic correction can be incorporated into this formalism.

7.2 Derivation of the wave equation.

We wish to show how the gyrokinetic correction, used in the derivation of chapter three, can be incorporated into the gyrokinetic formalism of the previous chapter. To illustrate the technique we shall consider the case of an isotropic plasma for which the perturbed Vlasov equation (7.26) simplifies considerably. For more complicated anisotropic distributions, however, the technique is the same.

Our starting point is, as in section 3.2, to express the field variables in terms of their Fourier transforms. For the field potential, for example, this gives us,

$$\delta\Phi = \int d^3\mathbf{k}\ \delta\Phi(\mathbf{k})\ \exp(i\mathbf{k}\bullet\mathbf{x}) \quad . \tag{7.32}$$

We now convert to gyrokinetic co-ordinates, expressing $\mathbf{k}$ as,

$$\mathbf{k} = k_{\parallel}\,\mathbf{e}_{\parallel} + k_{\perp}\,(\mathbf{e}_1 \cos\xi + \mathbf{e}_2 \sin\xi), \tag{7.33}$$

and so we have,

$$\delta\Phi_g = \int d^3\mathbf{k}\ \delta\Phi(\mathbf{k})\ \exp\left(i\mathbf{k}\bullet\mathbf{X} + i\frac{k_{\perp}u_{\perp}}{\Omega}\sin(\xi-\alpha)\right) \tag{7.34}$$

If we now assume that the initial distribution has a slow spatial variation and is isotropic (in other words we can approximate $F_{g0} = F_{g0}(\varepsilon)$) then equation (7.26) simplifies to,

$$\langle L_g \rangle_\ell \langle \delta H_g \rangle_\ell = - i\omega \frac{q}{m_0} \frac{\partial F_{g0}}{\partial \varepsilon} \langle \delta \psi_g \rangle_\ell , \tag{7.35}$$

where,

$$\delta \psi_g = \gamma \delta \Phi_g - \mathbf{u} \bullet \delta \mathbf{A_g} . \tag{7.36}$$

Noting that,

$$\begin{aligned} \mathbf{u} \bullet \delta \mathbf{A}(\mathbf{k}) &= u_\perp \, \delta A_1(\mathbf{k}) \cos \alpha + u_\perp \, \delta A_2(\mathbf{k}) \sin \alpha + u_\parallel \, \delta A_\parallel(\mathbf{k}) , \\ &= u_\perp \, \delta A_1(\mathbf{k}) \left[\cos (\xi - \alpha) \cos \xi + \sin (\xi - \alpha) \sin \xi \right] \\ &+ u_\perp \, \delta A_2(\mathbf{k}) \left[\cos (\xi - \alpha) \sin \xi + \sin (\xi - \alpha) \cos \xi \right] + u_\parallel \, \delta A_\parallel(\mathbf{k}) , \end{aligned} \tag{7.37}$$

our expression for $\delta \psi_g$ becomes,

$$\begin{aligned} \delta \psi_g = \int d^3\mathbf{k} \exp\left(i\mathbf{k} \bullet \mathbf{X} + i \frac{k_\perp u_\perp}{\Omega} \sin (\xi - \alpha) \right) \\ \times \Big\{ \left[\gamma \delta \Phi(\mathbf{k}) - u_\parallel \, \delta A_\parallel(\mathbf{k}) \right] \\ - u_\perp \left[\delta A_1(\mathbf{k}) \cos \xi + \delta A_2(\mathbf{k}) \sin \xi \right] \cos (\xi - \alpha) \\ - u_\perp \left[\delta A_1(\mathbf{k}) \sin \xi - \delta A_2(\mathbf{k}) \cos \xi \right] \sin (\xi - \alpha) \Big\} , \end{aligned} \tag{7.38}$$

with the ℓ^{th} Fourier component given by,

$$<\delta\psi_g>_\ell \;=\; \int d^3\mathbf{k}\, \exp\big(i\mathbf{k}\bullet\mathbf{X} \;+\; i\ell\xi\big)\, \Psi(\mathbf{k},\varepsilon,\mu;\mathbf{X})\,, \tag{7.39}$$

where,

$$\Psi(\mathbf{k},\varepsilon,\mu;\mathbf{X}) \;=\; \big[\gamma\delta\Phi(\mathbf{k}) - u_{\|}\,\delta A_{\|}(\mathbf{k})\big]\, J_\ell$$

$$-\frac{\ell\Omega}{k_\perp}\big[\delta A_1(\mathbf{k})\cos\xi + \delta A_2(\mathbf{k})\sin\xi\big]\, J_\ell$$

$$+\, u_\perp\big[\delta A_1(\mathbf{k})\sin\xi - \delta A_2(\mathbf{k})\cos\xi\big]\, iJ'_\ell\,, \tag{7.40}$$

the Bessel functions all have argument $k_\perp u_\perp/\Omega$ and the $\mathbf{X}$ dependence of Ψ is taken to be slow (that is, on a scale much less than the wavelength). This, then, provides us with our expression for the right hand side of equation (7.35). The right hand side is, from equation (7.27), the operator,

$$<L_g>_\ell = (u_{\|}\,\mathbf{e}_{\|} \;+\mathbf{u_D})\bullet\nabla_{\mathbf{X}} - i(\gamma\omega - \ell\Omega - \ell\omega_\alpha)\,, \tag{7.41}$$

acting on $<\delta H_g>_\ell$ which, for the isotropic distribution considered here, is simply, equal to $<\delta G_g>_\ell$. Solving, as in section 3.2, by the method of characteristics, gives us,

$$<\delta G_g>_\ell \;=\; -\,i\omega\,\frac{q}{m_0}\int d^3\mathbf{k}\,\exp(i\mathbf{k}\bullet\mathbf{X} + i\ell\xi)\int_0^\infty d\tau\,\exp(i(\gamma\omega - \ell\Omega - \ell\omega_\alpha)\tau\,)$$

$$\times\;\frac{\partial F_{g0}}{\partial\varepsilon}\;\Psi(\mathbf{k},\varepsilon,\mu;\mathbf{X}+\delta\mathbf{X}))\,\exp(i(\mathbf{k}\bullet\delta\mathbf{X} - \ell\,(\delta\Omega - \delta\omega_\alpha)\tau\,)\,, \tag{7.42}$$

where the co-ordinates preceded by δ are given by,

$$\frac{d}{d\tau}\delta\mathbf{X} = u_{\|}\,\mathbf{e}_{\|} + \mathbf{u_D}\,, \qquad \delta\mathbf{X}(\tau = 0) = \mathbf{0}\,, \tag{7.43}$$

that is, we are integrating backwards along the path of the gyrocentre. The gyrokinetic correction appears when we wish to convert this expression back into phase space co-ordinates. As the **X** variation in the integrand of the τ integral is assumed small, we may, in general, simply replace **X** by **x** throughout. However, in the rapidly varying resonant term this approximation is not sufficient and we must incorporate the gyrokinetic correction, by expanding the cyclotron frequency to first order in ρ/L, giving,

$$\gamma\omega - \ell\Omega - \ell\omega_\alpha = \gamma\omega - \ell\Omega_x - \frac{u_\perp}{\Omega}\,\ell\,(\nabla\Omega_x)_\perp \sin(\alpha - \beta) - \ell\omega_\alpha\,, \tag{7.44}$$

where $(\nabla\Omega_x)_\perp$ is the component of the cyclotron frequency gradient perpendicular to the field, and β is the angle the gradient makes with $\mathbf{e_1}$. Incorporating this into equation (7.42) results in the following expression for $\langle\delta G\rangle_\ell$,

$$\begin{aligned}\langle\delta G_g\rangle_\ell = & - i\omega\,\frac{q}{m_0}\int d^3\mathbf{k}\,\exp\Big(i\mathbf{k}\bullet\mathbf{x} - i\,\frac{k_\perp u_\perp}{\Omega}\sin(\xi - \alpha) + i\ell\xi\Big) \\ & \times \int_0^\infty d\tau\,\exp\Big(i\big(\gamma\omega - \ell\Omega - \frac{u_\perp}{\Omega}\,\ell\,(\nabla\Omega_x)_\perp \sin(\alpha - \beta) - \ell\omega_\alpha\big)\tau\Big) \\ & \times \frac{\partial F_{g0}}{\partial\varepsilon}\,\Psi(\mathbf{k},\varepsilon,\mu;\mathbf{x}+\delta\mathbf{x}))\,\exp\big(i(\mathbf{k}\bullet\delta\mathbf{x} - \ell\,(\delta\Omega - \delta\omega_\alpha)\tau\big)\,.\end{aligned} \tag{7.45}$$

When calculating the current density, we must integrate this function over α which will, in general, result in the two sine terms becoming series of Bessel functions, by way of the identity (3.13).

7.3 The O-mode with $k_y \neq 0$.

To illustrate the technique we derive the wave equation for the ordinary mode propagating perpendicular to the magnetic field, but at an angle ξ to the field gradient. For our co-ordinates we take $\mathbf{e_1}$ to lie in the direction of the field gradient and $\mathbf{e_2}$ as perpendicular to both the gradient and the direction of the magnetic field $\mathbf{e_\parallel}$. In this case, the perturbed field potential is zero and only the perpendicular component of the vector potential is non-zero. Expression (7.40) thus becomes simply,

$$\Psi(\mathbf{k},\varepsilon,\mu;\mathbf{X}) = u_\parallel \, \delta A_\parallel(\mathbf{k}) \, J_\ell \, . \tag{7.46}$$

As the co-ordinates are cartesian, the Vlasov operator also takes the simplified form,

$$\langle L_g \rangle_\ell = (u_\parallel \mathbf{e}_\parallel + \mathbf{u_D}) \bullet \nabla_{\mathbf{X}} - i(\gamma\omega - \ell\Omega) \, , \tag{7.47}$$

where,

$$\mathbf{u_D} = - \frac{u_\perp^2}{2\Omega L} \mathbf{e_2} \, , \tag{7.48}$$

is simply the gradient drift velocity. Our expression for $\langle \delta G \rangle_\ell$ thus becomes,

$$\begin{aligned} \langle \delta G \rangle_\ell = & - i\omega \frac{q}{m_0} \int d^3\mathbf{k} \exp(i\mathbf{k} \bullet \mathbf{x} - i \frac{k_\perp u_\perp}{\Omega} \sin(\xi - \alpha) + i\ell\xi) \\ & \times \int_0^\infty d\tau \exp(i(\gamma\omega - \ell\Omega + \frac{u_\perp}{L} \ell \cos\alpha)\tau) \frac{\partial F_0}{\partial \varepsilon} u_\parallel \, \delta A_\parallel(\mathbf{k}) \, J_\ell \, , \end{aligned} \tag{7.49}$$

where the effects of integrating along the path of the guiding centre have been ignored as they are of order ρ /L. We now form δF which is, from equations (7.19) and (7.23),

$$\delta F = - i\omega \frac{q}{m_0} \sum_{\ell = -\infty}^{\infty} \int d^3\mathbf{k} \exp(i\mathbf{k}\bullet\mathbf{x} - i \frac{k_\perp u_\perp}{\Omega} \sin(\xi - \alpha) + i\ell(\xi - \alpha))$$
$$\times \int_0^\infty d\tau \exp(i(\gamma\omega - \ell\Omega + \frac{u_\perp}{L} \ell \cos\alpha)\tau) \frac{\partial F_0}{\partial \varepsilon} u_\parallel \delta A_\parallel(\mathbf{k}) J_\ell + \delta F_a .$$

(7.50)

Integrating this over velocity space gives us the following expression for the perturbed current density,

$$\delta J = - i\omega \frac{q^2}{m_0} \sum_{\ell,m = -\infty}^{\infty} \int d^3\mathbf{u}\, \gamma \int d^3\mathbf{k} \exp(i\mathbf{k}\bullet\mathbf{x})\, u_\parallel \delta A_\parallel(\mathbf{k})\, J_\ell\, J_m \frac{\partial F_0}{\partial \varepsilon} \exp(i(\ell + m)\frac{\pi}{2})$$
$$\times \int_0^\infty d\tau \exp(i(\gamma\omega - \ell\Omega)\tau)\, J_{\ell+m}\left(\frac{u_\perp}{L} \ell\tau\right) - \varepsilon_0\omega_p^2 \delta A_\parallel . \qquad (7.51)$$

The arguments of the first two Bessel functions are, once again, $k_\perp u_\perp/\Omega$. The presence of the three Bessel functions will, usually, make it impossible to perform the velocity integrals. However, we may simply expand them for a given resonance. For the fundamental ($\ell = 1$), for example, we need expand to second order (requiring the m = -1 and m= 0 terms) to give,

$$\delta J = - i\omega \frac{q^2}{m_0} \int d^3\mathbf{u}\, \gamma \int d^3\mathbf{k} \exp(i\mathbf{k}\bullet\mathbf{x})\, u_\parallel \delta A_\parallel(\mathbf{k}) \frac{\partial F_0}{\partial \varepsilon}$$
$$\times \int_0^\infty d\tau \exp(i(\gamma\omega - \ell\Omega)\tau) \left(- \frac{k_\perp^2 u_\perp^2}{4\Omega^2} + i \frac{k_\perp u_\perp^2 \tau}{2\Omega L} \exp(-i\frac{\pi}{2}) \right) - \varepsilon_0\omega_p^2 \delta A_\parallel .$$

(7.52)

If we now assume a Maxwellian distribution, the velocity and τ integrals can be performed (by the same technique as chapter 3), to give,

$$\delta J = \frac{\mu_0}{2}\frac{\omega_p^2}{\Omega_0^2} \int d^3\mathbf{k}\, \exp(i\mathbf{k}\bullet\mathbf{x})\, \delta A_\parallel(\mathbf{k})$$

$$\times \left(- k_\perp^2 F_{7/2} + i \frac{\mu k_\perp}{L} \exp(-i\frac{\pi}{2}) \frac{dF_{7/2}}{d\xi} \right) - \varepsilon_0 \omega_p^2 \delta A_\parallel . \qquad (7.53)$$

where the relativistic dispersion functions have argument $\xi = \mu\,(1 - \Omega/\omega)$. Inverting the Fourier transforms and substituting in Maxwell's equations, we have our final equation,

$$\frac{d}{dx}\left\{ \left[1 + \frac{1}{2}\frac{\omega_p^2}{\Omega_0^2} F_{7/2} \right] \frac{d\delta A_\parallel}{dx} \right\}$$

$$+ \left(- k_y^2 + \frac{1}{2}\frac{\omega_p^2}{\Omega_0^2} \left[- k_y^2 F_{7/2} + k_y \frac{dF_{7/2}}{dx} \right] + \frac{\omega^2 - \omega_p^2}{c^2} \right) \delta A_\parallel = 0 ,$$

(7.54)

8. CONCLUSION.

Chapters two to seven contain the core of this thesis, namely the discussion of the propagation of plasma waves through electron cyclotron resonances with regards to the radio frequency heating of plasmas. In chapter nine we shall look at the different, and yet related, problem of synchrotron radiation instabilities in runaway electrons in tokamaks. Before doing so we shall, in this chapter, collect together the ideas expressed so far.

The propagation of plasma waves through a resonance may be explained by a variety of different methods of which the method of this thesis, direct integration of the full wave equations, is just one. We may group these approaches as single mode, contour integration and full wave integration.

Single mode methods, such as WKB theory, begin with the assumption that there is little interaction between the wave modes of the plasma and each mode can be analysed separately. In section 4.1 we illustrated how to solve the full wave equations by taking a single mode approximation (essentially by replacing the spatial derivatives with ik's) and showed the resulting equations to be consistent with WKB theory. This is the case for all the equations of chapter 4. Despite describing wave absorption, such techniques offer no information on reflection and mode conversion, as such processes involve the exchange of energy between two wave modes. Techniques are available, though, for incorporating such processes into a WKB analysis in terms of linear mode conversion (Littlejohn and Flynn (1993)). However, because reflection and mode conversion are localised, almost exclusively, to regions of resonance, single mode theory provides a good description of wave propagation in the majority of the plasma. Beskin et al (1987) provide a theory for such propagation through inhomogeneous plasmas.

Contour integration involves the solution of the full wave equation in terms of an integral in the complex plane (Swanson (1978)). Such a solution requires an expansion of the wave dispersion functions about the resonance. Contour integration can explain effects such as mode conversion and reflection. Such an analysis, including the gyrokinetic correction, was performed by Antonsen and Manheimer (1978) but in neglecting higher order effects of the relativistic dispersion relation their work tended to place too much emphasis on mode conversion to Bernstein waves, over absorption. For example, they predicted that at the second harmonic resonance with high field incidence, energy would not be absorbed but rather completely converted to the Bernstein mode. Our analysis has shown this not to be the case. However, higher order effects of the relativistic dispersion functions may be incorporated into such analyses (Swanson (1978)) and it would be of interest to compare such a method with full wave equations.

Full wave equations for electron cyclotron resonance have been derived by a number of authors. Maroli et al (1986), Petrillo et al (1987) and Lampis et al (1987) derived and solved such equations for the fundamental and first harmonic resonances including, although not explicitly, the gyrokinetic correction. In this work we have given a simplified derivation for such equations. Our basis has been the work of Cairns et al (1991), an analysis which did not include the relativistic effects known to be of importance. Consequently, their wave equations did not describe relativistic broadening but can be seen as the low temperature limit of the relativistic full wave equations given in chapter 4. Extending the technique of Cairns et al (1991) into the relativistic regime we have been able to reproduce the equations of Maroli et al (1986), Petrillo et al (1987) and Lampis et al (1987) by a much simpler method.

A similar technique can also be applied to ion cyclotron heating (Brambilla (1989), Cairns et al (1991), Holt et al (1992) and Sauter and Vaclavik (1992)). Here we have the simplification that we no longer need consider relativistic effects, but the

complication that we can no longer expand in kρ as this parameter may be large. This results in systems of integro-differential equations which are much more difficult to solve numerically. However, methods - such as fast wave theory (Kay et al (1988) and Lashmore-Davies et al (1988)) - are available to simplify their solution.

For more complicated geometries, we have shown, in chapter 7, how the gyrokinetic correction can be incorporated into the relativistic gyrokinetic formalism of Tsai et al (1984). The derivation of relativistic full wave equations for more complicated geometries has been carried out by van Bruggen-Kerkhof (1992), although their equations do not include the gyrokinetic correction and may not be energy conserving.

Numerically, we have shown that wave absorption is in close agreement with WKB theory for the O-mode at the fundamental and the X-mode at the second harmonic. For the X-mode at the first harmonic, though, we have seen a large absorption for high field propagation which is not predicted by WKB theory. This is due to the conversion of the X-mode to the Bernstein mode at the upper-hybrid resonance.

9. RUNAWAY ELECTRON INSTABILITIES.

During many tokamak disruptions a large number of high energy electrons (runaways) are produced. Runaways can cause damage to the tokamak through impacting on the sides of the containment vessel, and so it is important to gain an understanding of their behaviour. In particular, it is known that runaways have a decay time much shorter than would be predicted from energy loss by synchrotron radiation, and so we would like to suggest an alternative mechanism (Lashmore-Davies and McDonald (1994)).

9.1 Experimental Evidence.

Disruptions in tokamaks lead to a drop in the bulk temperature of the plasma with some of the lost energy going into the production of high energy electrons (runaways). A good account of this is given, for the JET tokamak, by Wesson et al (1989). They describe how, in the aftermath of some MHD disruptions, much of the plasma current can be carried from the bulk plasma to the runaways, and this current can be transferred to the containment vessel of the tokamak resulting in large forces of the order of hundreds of tonnes. Observation of runaways in Tore Supra (Chatelier et al (1989)) and more recently in JET (Gill (1993)) have suggested that we are still some way from understanding their nature.

Gill (1993) gave the following values (Table (9.1)) for a post disruption plasma.

9. RUNAWAY ELECTRON INSTABILITIES.

During many tokamak disruptions a large number of high energy electrons (runaways) are produced. Runaways can cause damage to the tokamak through impacting on the sides of the containment vessel, and so it is important to gain an understanding of their behaviour. In particular, it is known that runaways have a decay time much shorter than would be predicted from energy loss by synchrotron radiation, and so we would like to suggest an alternative mechanism (Lashmore-Davies and McDonald (1994)).

9.1 Experimental Evidence.

Disruptions in tokamaks lead to a drop in the bulk temperature of the plasma with some of the lost energy going into the production of high energy electrons (runaways). A good account of this is given, for the JET tokamak, by Wesson et al (1989). They describe how, in the aftermath of some MHD disruptions, much of the plasma current can be carried from the bulk plasma to the runaways, and this current can be transferred to the containment vessel of the tokamak resulting in large forces of the order of hundreds of tonnes. Observation of runaways in Tore Supra (Chatelier et al (1989)) and more recently in JET (Gill (1993)) have suggested that we are still some way from understanding their nature.

Gill (1993) gave the following values (Table (9.1)) for a post disruption plasma.

Table 9.1.

Parameters for JET Disruptions Observed by Gill (1993).

Magnetic field	2.7 T
Magnetic field length scale	3 m
Thermal electrons:	
Density	2×10^{19} m^{-3}
Temperature	25eV - 50eV
Runaways:	
Current	1 MA
Energy	35 MeV
Density	2×10^{16} m^{-3}
Decay Time	2 s

Clearly, the bulk temperature of the plasma has fallen considerably from its operational temperature (around 10 keV) with much of the lost energy being transferred to the runaways. The large energies of the runaways make them highly relativistic with a relativistic mass increase of $\gamma = 70$.

Of particular interest is the decay time of the runaways. We would expect the runaways' energy to decay as a result of synchrotron radiation through orbiting the tokamak, a process with a decay time given, from Gill (1993), by,

$$\tau = 177\, R^2/\beta^3\gamma^3 , \qquad (9.1)$$

where R is the major radius of the tokamak and β is the speed of the runaways scaled to the speed of light. For JET (Table (9.1)) this would suggest an energy loss time of $\tau = 73$ s which is clearly way too slow to account for the observed loss time of 2 s. Energy loss

must then be due to an additional mechanism which either leads directly to energy loss or converts some of the runaways' parallel energy to perpendicular energy which will then cause decay through the emission of cyclotron radiation. If the runaways had a pitch angle, α, to the magnetic field, B, then the energy emitted by cyclotron radiation would be, also from Gill (1993),

$$\tau = 3 \times 10^8/\gamma B^2\beta^2\sin^2\alpha \,, \tag{9.2}$$

which for an angle of the order of a few degrees would give energy loss times of the correct size.

We shall now look at the interaction between the runaways and the thermal electrons of a post disruption plasma, by forming the dispersion relation of a relativistic beam in a hot background plasma.

9.2 The Dispersion Relation.

We wish to derive then, the dispersion relation for a relativistic beam of electrons in hot plasma. Our analysis will be an extension of that of Zayed and Kitsenko (1968), who studied the case of a relativistic beam in a cold plasma. We follow these authors by assuming the distribution function of the runaways to be,

$$f_{0b} = \frac{n_{0b}}{2p_{\perp 0}} \delta(p_\perp - p_{\perp 0}) \, \delta(p_z - p_{z0}) \,. \tag{9.3}$$

Zayed and Kitsenko (1968) showed that for the above distribution function the ordinary and extraordinary waves are both unstable at the fundamental and harmonics of the electron cyclotron frequency for perpendicular propagation. They also showed that

obliquely propagating waves can be unstable. However, since these authors assumed a cold background plasma they did not include the important effects of cyclotron damping by the background plasma or equivalently, mode coupling to cyclotron harmonic waves (Cairns and Lashmore-Davies (1982)) supported by the background plasma. In order to include these effects, a hot background plasma must be used. We therefore combine the dielectric tensor for the relativistic, gyrating electrons, given by Zayed and Kitsenko (1968), with the standard dielectric tensor for a hot background plasma in which the bulk electrons have a Maxwellian distribution (Equation (2.9)). Here, we shall confine our attention to the case of the ordinary mode propagating perpendicular to a uniform magnetic field in a uniform plasma. For this case the dispersion relation is,

$$\frac{k^2c^2}{\omega^2} = 1 - \frac{\omega_{pe}^2}{\omega}\exp(-\lambda)\sum_{n=-\infty}^{\infty}\frac{I_n(\lambda)}{\omega - n\Omega_e}$$

$$- \frac{\omega_{pb}^2}{\omega^2} - \sum_{l=-\infty}^{\infty}\frac{v_{z0}^2}{v_{\perp 0}^2}\omega_{pb}^2\frac{2kv_{\perp 0}}{\Omega_b}\frac{J_l(kv_{\perp 0}/\Omega_b)\,J_l'(kv_{\perp 0}/\Omega_b)}{\omega(\omega - l\Omega_b)}$$

$$+ \sum_{l=-\infty}^{\infty}\frac{v_{z0}^2}{c^2}\omega_{pb}^2\frac{J_l^2(kv_{\perp 0}/\Omega_b)}{(\omega - l\Omega_b)^2}\,, \qquad (9.4)$$

where,

$$\lambda = k^2\rho^2/2\,, \quad \rho = v_t/\Omega_e\,, \quad \Omega_e = \frac{B_0\,q}{m_0}, \quad \Omega_b = \frac{B_0\,q}{\gamma_b\,m_0},$$

$$\omega_{pe}^2 = \frac{n_{0e}\,q^2}{\varepsilon_0 m_0}, \qquad \omega_{pb}^2 = \frac{n_{0b}\,q^2}{\varepsilon_0\,\gamma_b\,m_0}$$

and $\gamma_b = (1 - v_{z0}^2/c^2 - v_{\perp 0}^2/c^2)^{-1/2}$ is the relativistic mass increase of the runaways. Throughout, we are using the subscript 'e' for the background (thermal) electrons, and the subscript 'b' for the runaway (beam) electrons.

We begin by studying the behaviour of the dispersion relation near the m^{th} cyclotron harmonic of the runaways far from any resonance with the thermal electrons. This was the case dealt with by Zayed and Kitsenko (1968) and can be described by taking the cold plasma limit of the thermal plasma (i.e. ignoring the first summation on the RHS), together with the resonant component of the beam response, given by the m^{th} component of the final term on the RHS (the second term on the RHS generally being negligible). The resulting dispersion relation is,

$$(\omega^2 - \omega_{pe}^2 - \omega_{pb}^2 - k^2c^2)(\omega - m\Omega_b)^2 + \frac{v_{z0}^2}{c^2}\omega_{pb}^2\,\omega^2\,J_m^2 = 0\,, \qquad (9.5)$$

which represents the positive energy cold plasma wave together with two negative energy cyclotron modes. Looking at the behaviour of the cyclotron modes, by expanding the frequency $\omega = \omega_0 + \delta\omega$ about $\omega_0 = m\Omega_b$, we have,

$$(\omega_0^2 - \omega_{pe}^2 - \omega_{pb}^2 - k^2c^2)(\delta\omega)^2 + \frac{v_{z0}^2}{c^2}\omega_{pb}^2\,\omega_0^2\,J_m^2 = 0\,. \qquad (9.6)$$

Clearly, for any given value of the wave number k, if the frequency of the wave lies below that of the cold plasma mode then $(\delta\omega)^2$ is positive and the modes are stable. This means that harmonics below the plasma frequency will be stable, and so imposes a lower limit on unstable harmonics,

$$n^2 > \frac{\omega_{pe}^2 + \omega_{pb}^2}{\Omega_b^2}\,. \qquad (9.7)$$

For typical JET parameters this gives $n \geq 38$, indicating that the instability of the ordinary mode is shifted to very high harmonics characteristic of synchrotron radiation (see for example Feynman (1965) or Bekefi (1966)). Alternatively, if the frequency lies above that of the cold plasma mode then $(\delta\omega)^2$ is negative and the modes form conjugate pairs one of which will be unstable. As one would expect then, the dispersion relation goes unstable when the resonances become degenerate at $\omega_0 = (\omega_{pe}^2 + \omega_{pb}^2 + k^2c^2)^{1/2} = m\Omega_b$, expanding about which gives us,

$$2\,\omega_0\,(\delta\omega)^3 + \frac{v_{z0}^2}{c^2}\,\omega_{pb}^2\,\omega_0^2\,J_m^2 = 0\,, \tag{9.8}$$

which does indeed have an unstable solution. The dispersion relation is illustrated in Fig. (9.1) and we can see that at each mode degeneracy the upper cyclotron mode couples with the cold plasma wave to produce a reactive instability.

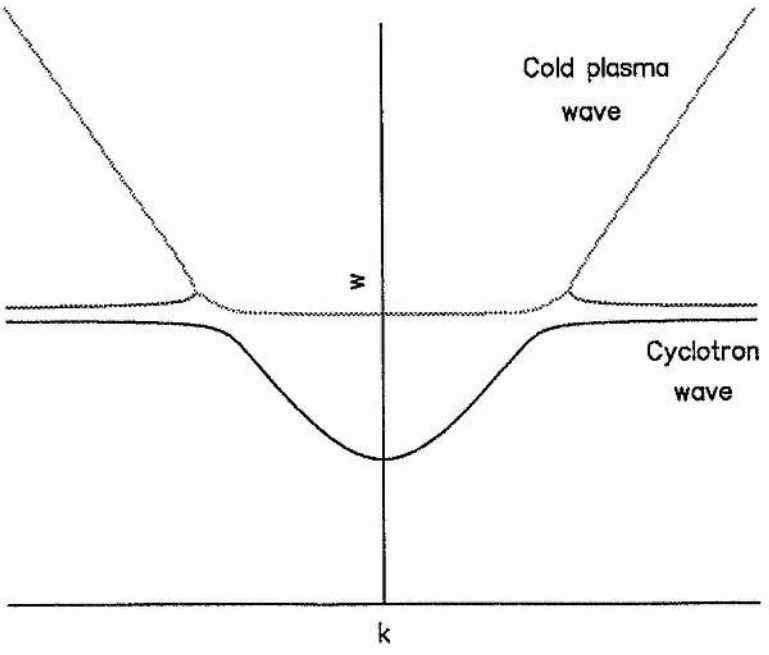

Figure 9.1

Dispersion relation for one cyclotron harmonic.

We now wish to consider the effect of the thermal plasma on the runaways. To do this we shall begin by looking at the special case in which the cyclotron frequency of the thermal electrons is resonant with a harmonic of the runaways, $\Omega_e = m\Omega_b$ or in other words $\gamma_b = m$. In this case we must also include the contribution from the first harmonic of the thermal electrons (the n=1 term in the first summation of equation (9.4), which we shall expand to order $k^2\rho^2$), so we now have,

$$(\omega^2 - \omega_{pe}^2 - \omega_{pb}^2 - k^2c^2) + \frac{v_{z0}^2}{c^2}\omega_{pb}^2\,\omega^2\frac{J_m^2}{(\omega - m\Omega_b)^2} - \omega_{pe}^2\,\omega\frac{\frac{1}{2}\lambda}{\omega - \Omega_e} = 0\,. \tag{9.9}$$

Expanding this about the resonance point, $\omega_0 = (\omega_{pe}^2 + \omega_{pb}^2 + k^2c^2)^{1/2} = m\Omega_b = \Omega_e$, gives,

$$(\delta\omega)^3 - \tfrac{1}{4}\lambda\,\omega_{pe}^2\,(\delta\omega) + \tfrac{1}{2}\frac{v_{z0}^2}{c^2}\omega_{pb}^2\,\omega_0\,J_m^2 = 0\,. \tag{9.10}$$

We now have an instability with a threshold resulting from the stabilising effect of the thermal electrons. The condition for instability is (after dividing through by Ω_e^6),

$$(\tfrac{1}{2}\frac{v_{z0}^2}{c^2}\frac{\omega_{pb}^2}{\Omega_e^2}J_m^2)^2 > \frac{4}{27}(\tfrac{1}{4}\lambda\frac{\omega_{pe}^2}{\Omega_e^2})^3\,. \tag{9.11}$$

For the values given by Gill (1993) we find the left hand side is $2.0 \times 10^{-14}\,J_m^4(m\tan\alpha)$ (where α is the pitch angle of the runaways) and the right hand side is 1.8×10^{-17}. No

values for the pitch angle of the runaways were given, but taking the most unstable case ($\alpha = \pi/4$) and noting the relation,

$$J_m(m) \sim \frac{\Gamma\left(\frac{1}{3}\right)}{48^{1/6}\,\pi\, m^{1/3}}, \tag{9.12}$$

(Abramowitz and Stegun (1965)) we see that for the first harmonic above the cutoff (n=38) the LHS becomes 6.4×10^{-18}. Even in this case then, when the destabilising effects are at their greatest, the resonance with the thermal electrons removes the instability. Harmonics away from the thermal plasma cyclotron resonance will remain unstable though and propagate through the plasma.

The optical depth of the plasma,

$$\tau = \frac{\pi}{2}\,\frac{\omega_{pe}^2}{\Omega_{0e}}\,\frac{L}{\mu c}\left(1 - \frac{\omega_{pe}^2}{\Omega_{0e}^2}\right)^{1/2}, \tag{9.13}$$

(from equation (4.17)) will be small ($\tau \sim 0.1$, for typical JET parameters), as a result of the low post-disruption temperature of the thermal electrons. As a result, reabsorption of the radiation produced by the beam-plasma instabilities will not be a significant factor.

9.3 Discussion.

We have discussed the production and possible consequences of runaway electrons in a tokamak and, in particular, have identified the problem of their relatively fast energy loss times. A possible mechanism for increasing the rate of energy loss is through a synchrotron instability of the runaways and we have shown, through studying a relativistic electron beam in a hot magnetised plasma, how such instabilities can exist.

The highly relativistic ($\gamma >> 1$) nature of the runaway electrons results in their low harmonics being below the thermal plasma frequency and, as a result, being stabilised by it. Higher harmonics, though, are unstable and could result in much enhanced synchrotron radiation which would account for the observed fast energy loss times of the runaways. It should be noted that here we have only discussed the special case of the ordinary mode for perpendicular propagation. We would also expect the extraordinary mode and obliquely propagating modes to be unstable (Zayed and Kitsenko (1968)) and their effects would also be significant.

A further case for consideration is the interaction of the runaways with lower frequency modes. The large downshift in the cyclotron frequency of the runaways brings it towards the lower hybrid frequency of the thermal plasma,

$$\omega_{LH}^2 = \frac{\omega_{pi}^2 \, \Omega_{0e}^2}{\omega_{pe}^2 + \Omega_{0e}^2} \, , \tag{9.14}$$

(see for example Stix (1992)) which for the parameters given by Gill (1993) (Table (9.1)) gives us $\omega_{LH} = 5.8 \times 10^9$ rads^{-1}. Consequently, the fundamental harmonic of the runaways may be unstable through its interaction with the lower hybrid wave.

An alternative mechanism, for energy loss from runaways, was given by Laurent and Rax (1990), who suggested that the runaways were destabilised by a non-linear interaction with the variations in the toroidal magnetic field due to finite number of field coils (toroidal ripple). Their analysis, however, did not consider the effect of the background plasma and it would be interesting to see what effect its inclusion (a similiar calculation was performed by Lashmore-Davies (1990) for the low frequency case) would have.

APPENDIX: SPECIAL FUNCTIONS.

The Bessel functions and Plasma Dispersion functions are used throughout this work and some of their properties, those relevant to the derivations and discussions, are given here for ease of reference.

A.1 Bessel Functions.

Bessel functions are used throughout the derivation in chapter 3 and the resulting general wave equation (3.23) is expressed in terms of modified Bessel functions, both of which are defined in Abramowitz and Stegun (1965). All Bessel functions used are of integer order and hence in the relations given below the order (n) is taken as an integer.

A.1.1 Fourier Series.

The Fourier components of the expression $\exp(ib\sin\theta)$ are the Bessel functions J_n, a result which can be expressed as,

$$e^{ib\sin\phi} = \sum_{m=-\infty}^{\infty} J_m(b)\, e^{im\phi}. \qquad (A.1)$$

This identity is quoted, where it is first used, in section 3.2 as equation (3.13). By differentiating it, with respect to b and ϕ respectively, we obtain the two further relations,

$$\cos\phi\, e^{ib\sin\phi} = \sum_{m=-\infty}^{\infty} \frac{n}{b} J_m(b)\, e^{im\phi}, \qquad (A.2)$$

$$\sin\phi\, e^{ib\sin\phi} = \sum_{m=-\infty}^{\infty} \left(-i\, J_m'(b) \right) e^{im\phi}, \qquad (A.3)$$

both of which are also used for expanding out (3.12) and (3.18).

A.1.2 Integral Identities.

To perform the $U_\perp$ integrals in (3.22) requires the following relation,

$$\int_0^\infty dx\, J_n(ax)\, J_n(bx)\, x \exp(-x^2) = \frac{1}{2} I_n \exp\left(-\frac{a^2+b^2}{4} \right), \qquad (A.4)$$

where the modified Bessel function has argument ab/2, along with two other identities derived from it. Firstly, if we differentiate (A.4) with respect to a we find that,

$$\int_0^\infty dx\, J_n'(ax)\, J_n(bx)\, x^2 \exp(-x^2) = \frac{1}{2}\left[\frac{b}{2} I_n' - \frac{a}{2} I_n' \right] \exp\left(-\frac{a^2+b^2}{4} \right). \qquad (A.5)$$

Secondly, if we differentiate (A.5) with respect to b we have,

$$\int_0^\infty dx\, J_n'(ax)\, J_n'(bx)\, x^3 \exp(-x^2) = \frac{1}{2}\left[\left(\frac{ab}{2} + \frac{n^2}{ab} \right) I_n - \frac{a^2+b^2}{4} I_n' \right] \exp\left(-\frac{a^2+b^2}{4} \right). \qquad (A.6)$$

Once more, it should be noted that the modified Bessel functions in (A.5) and (A.6) all have argument ab/2.

A.1.3 Small Argument Expansions.

In chapter 4 the general wave equation (3.23) is expanded in the parameter ε to produce differential wave equations. To do this it is necessary to know the small argument expansions of the modified Bessel functions.

The general power series expansion of a modified Bessel function of integer order, is, from Abramowitz and Stegun (1965),

$$I_n(x) = \sum_{m=-\infty}^{\infty} \frac{1}{j!\,(n+j)!} \left(\frac{x}{2}\right)^{n+2j} . \tag{A.7}$$

From this we may take the following expansions, relevant in chapter 4,

$$I_0(x) = 1 + \frac{x^2}{4} + \ldots , \tag{A.8}$$

$$I_1(x) = \frac{x}{2} + \frac{x^3}{16} + \ldots , \tag{A.9}$$

$$I_2(x) = \frac{x^2}{8} + \ldots , \tag{A.10}$$

and their derivatives,

$$I_0'(x) = \frac{x}{2} + \ldots , \tag{A.11}$$

$$I_1'(x) = \frac{1}{2} + \frac{3x^2}{16} + \ldots , \tag{A.12}$$

$$I_2'(x) = \frac{x}{4} + \ldots . \qquad (A.13)$$

A.2 Relativistic Plasma Dispersion Functions.

The results quoted here are all taken from the excellent discussion paper, on the properties of the relativistic plasma dispersion function (RPDF), of Robinson (1986). The RPDF's used in this thesis all have real arguments and half-integer subscript which we shall assume to be the case in the following identities.

A.2.1 Definitions.

The Shkarofsky function is defined as,

$$\mathfrak{F}_q(z,a) = -i\int_0^\infty dt \frac{1}{(1 - it)^q} \exp\left(izt - \frac{at^2}{1 - it}\right). \qquad (A.14)$$

Qualitatively, it represents absorption with a profile which is partly due to relativistic mass broadening - which has a quadratic velocity dependence and is identified with the first (z) argument - and partly due to the Doppler broadening - which has a linear velocity dependence and is identified with the second (a) argument.

If Doppler broadening is not present then we have the Dnestrovskii function, given by,

$$F_q(z) = \mathfrak{F}_q(z,0). \qquad (A.15)$$

Further, the generalised Dnestrovskii function is given by,

$$\mathfrak{F}_{q,m}(z,a) = \frac{\partial^m \mathfrak{F}_q(z,a)}{\partial z^m}. \qquad (A.16)$$

A.2.2 Relations.

The asymptotic behaviour of the generalised Dnestrovskii functions for large argument is,

$$\mathfrak{F}_q(z,a) \sim \frac{1}{z-a}. \qquad (A.17)$$

The absorption profile due to the RPDF's is given by the imaginary part of the functions which, for the Dnestrovskii functions is given by,

$$\text{Im } F_q(x) = \begin{cases} 0, & x \le 0, \\ -\pi (-x)^{q-1} e^x / \Gamma(q), & x \ge 0. \end{cases} \qquad (A.18)$$

In chapter 6 this result is used to calculate the absorption across the plasma.

In chapter 4, we require the identity,

$$\mathfrak{F}_q(z,a) \sim \tfrac{1}{2} a^{-1/2} Z\left(\tfrac{1}{2} z\, a^{-1/2}\right), \qquad (A.19)$$

for $z \ll a$ and $a \gg 1$, to derive the result (4.19).

REFERENCES

Abramowitz M. and Stegun I. A., Handbook of Mathematical Functions, Dover, (1965).

Antonsen T. M. and Manheimer W. M., Phys. Fluids **21** (1978) 2295.

Bekefi G., Radiation Processes in Plasmas, John Wiley, (1966).

Beskin V. S., Gurevich A. V. and Istomin Ya. I., Sov. Phys. JETP **65** (1987) 715.

Bornatici M., Proc. 18th European Conference on Cont. Fus. and Plasma Phys. **3**, 257, Berlin (1991).

Bornatici M., R. Cano, O. De Barbieri and F. Engelmann, Nuc. Fus. **23** (1983) 1153.

Brambilla M., Plasma Phys. and Cont. Fus. **31** (1989) 723.

van Bruggen-Kerkhof M. J., PhD Thesis (1992).

Cairns R. A. and Lashmore-Davies C. N., Phys. Fluids **25** (1982) 1605.

Cairns R. A., Plasma Physics, Blackie, (1985).

Cairns R. A., C. N. Lashmore-Davies, R. O. Dendy, B. M. Harvey, R. J. Hastie and H. Holt, Phys. Fluids B **3** (1991) 2953.

Cairns R. A., Radiofrequency Heating of Plasmas, Adam Hilger, (1991).

Chatelier M. et al, Proc. XVI EPS Conference on Cont. Fus. and Plasma Phys., Venice (1989).

Chen L. and Tsai S., Phys. Fluids **26** (1983) 141.

Chen L., Waves and Instabilities in Plasmas, World Scientific, (1987).

Dnestrovskii Y. N., Kostomarov D. P. and Skrydlov N. V., Sov. Phys. Tech. Phys. **8** (1964) 691.

Efthimion P. C., Arunasalam V. and Hosea J. C., Phys. Rev. Letters **44** (1980) 396.

Feynman R. P., Lecture Notes in Physics ,Vol.1, Addison-Wesley, (1965).

Gill R. D., Nuc. Fus. **33** (1993) 1613.

Holt H., Cairns R. A., and Lashmore-Davies C. N., Proc. 19th Europhysics Topical Conference on RF Heating and Current Drive of Fus., 25, European Physical Society, Brussels (1992).

Kay A., Cairns R. A. and Lashmore-Davies C. N., Plasma Phys. Cont. Fus. **30** (1988) 471.

Kreischer K. E., Danly B. G., Saito H., Schutkeker J. B., Temkin R. E. and Tran T. M. Plasma Phys. Cont. Fus. **27** (1985) 1449.

Lampis G., Maroli C. and Petrillo V., Plasma Phys. and Cont. Fus. **29** (1987) 1137.

Lashmore-Davies C. N., Fuchs V., Francis G., Ram A. K., Bers A. and Gauthier L., Phys. Fluids **31** (1988) 1614.

Lashmore-Davies C. N. and Dendy R. O., Phys. Fluids B **1** (1989) 1565.

Lashmore-Davies C. N., Plasma Phys. and Cont. Fus. **32** (1990) 1115.

Lashmore-Davies C. N. and McDonald D. C., Accepted by Physica Scripta.

Laurent L. and Rax J. M., Europhys. Letters **11** (1990) 219 .

Littlejohn R. G. and Flynn W. G., Phys. Rev. Lett. **70** (1993) 1799.

McDonald D. C., Cairns R. A. and Lashmore-Davies C. N., Phys. Plasmas **1** (1994) 842.

Maroli C., Petrillo V., Lampis G. and Engelmann F., Plasma Phys. and Cont. Fus. **28** (1986) 615.

Maroli C., Petrillo V. and Lampis G., Plasma Phys. and Cont. Fus. **30** (1988) 1723.

Pachtman A., Wolfe S. M. and Hutchinson I. H., Nuc. Fus. **27** (1987) 1283.

Petrillo V., Lampis G. and Maroli C., Plasma Phys. and Cont. Fus. **29** (1987) 877.

Robinson P. A., J. Math. Phys. **27** (1986) 1206.

Robinson P. A., J. Math. Phys. **28** (1987) 1203.

Rutherford P. H. and Frieman E. A., Phys. Fluids **11** (1968) 569.

Sauter O., and Vaclavik J., Nuc. Fus. **32** (1992) 1455.

Shkarofsky I. P., Phys. Fluids **9** (1966) 561.

Shohet J., Comm. Plasma Phys. Cont. Fus. **4** (1978) 37.

Smith R. J., Bartlett D. V., Costley A. E. and Richards R. A., Proc. EC-8 Workshop, Gut Ising (1992).

Stix T. H., Waves in Plasmas, American Institute of Physics, (1992).

Swanson D. G., Phys. Fluids **21** (1978) 926.

Swanson D. G., Phys. Fluids **28** (1985) 2645.

Swanson D. G., Plasma Waves, Academic Press, (1989).

Taylor J. B. and Hastie R. J., Plasma Phys. **10** (1968) 479.

TFR Team, Proc. 8th Internat. Conf. on Plasma Phys. and Cont. Fus. research, Brussels (1980).

Tsai S. T., Van Dam J. W. and Chen L., Plasma Phys. and Cont. Fus. **26** (1984) 907.

Wesson J. A. et al, Nuc. Fus. **29** (1989) 641.

White R. B., Theory of Tokamak Plasmas, North-Holland, (1989).

Zayed K. A. and Kitsenko A. B., Plasma Phys. **10** (1968) 147.